Nuclotron based Ion Colider fAcility

Scientific report
"Experimental programme at MPD"

V. Riabov for the MPD Collaboration

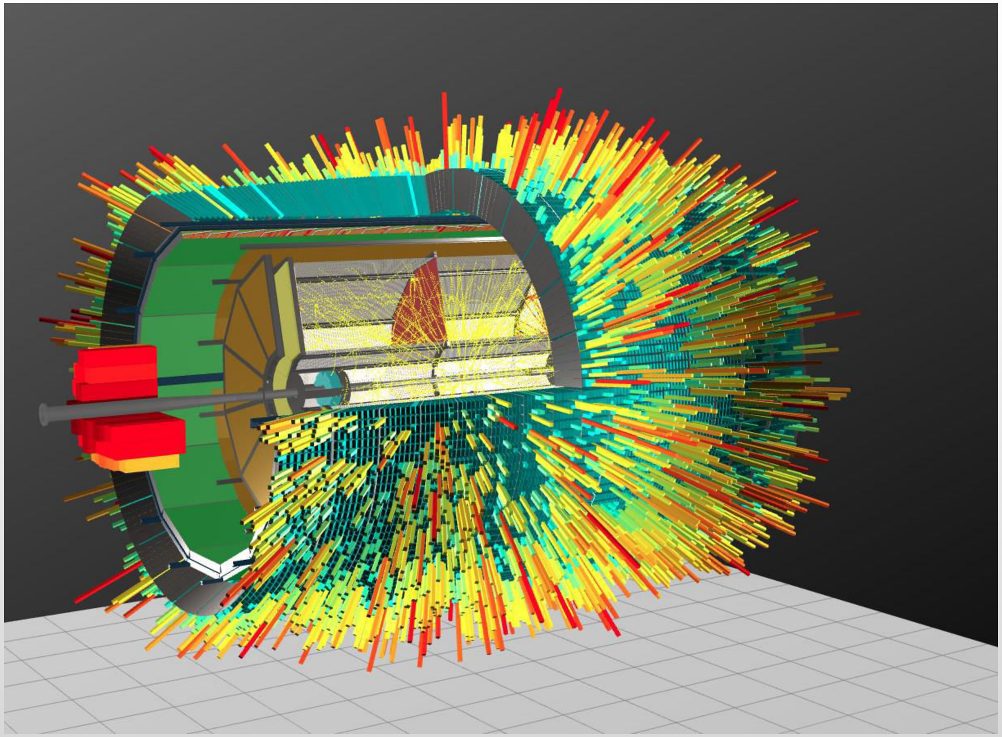

MPD at NICA

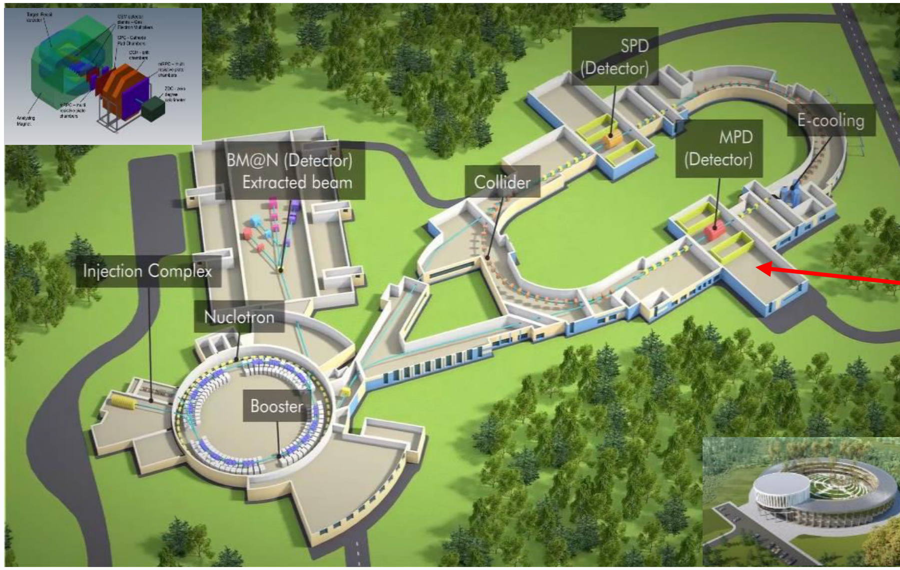

Stage- I

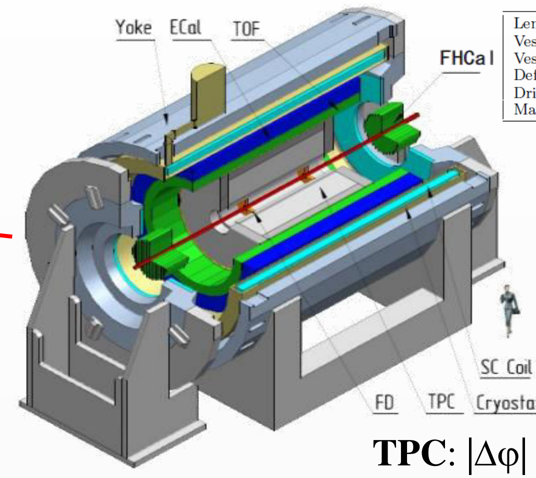

Length	340 cm
Vessel outer radius	140 cm
Vessel inner radius	27 cm
Default magnetic field	0.5 T
Drift gas mixture	90% Ar+10% CH_4
Maximum event rate	7 kHz ($L = 10^{27}$ $cm^{-2}s^{-1}$)

TPC: $|\Delta\varphi| < 2\pi$, $|\eta| \leq 1.6$
TOF, EMC: $|\Delta\varphi| < 2\pi$, $|\eta| \leq 1.4$
FFD: $|\Delta\varphi| < 2\pi$, $2.9 < |\eta| < 3.3$
FHCAL: $|\Delta\varphi| < 2\pi$, $2 < |\eta| < 5$

- One of two collider experiments at NICA collider to study heavy-ion collisions at $\sqrt{s_{NN}}$= 4−11 GeV
- Expected beam configuration in Stage-I:
  - ✓ not-optimal beam optics with wide z-vertex distribution, σ_z ~ 50 cm
  - ✓ reduced luminosity (~10^{25} is the goal for 2023) → collision rate ~ 50 Hz
  - ✓ collision system available with the current sources: C (A=12), N (A=14), Ar (A=40), Fe (A=56), Kr (A=78-86), Xe (A=124-134), Bi (A=209) → start with Bi+Bi @ 9.2 GeV in 2023-2024

MPD status and plans

- ❖ 2022:
  - ✓ preparation of the SC magnet for cooling
- ❖ 2023:
  - ✓ cooling the magnet and MF measurement
  - ✓ installation of the support frame and detectors
- ❖ 2024:
  - ✓ MPD commissioning
  - ✓ first run with BiBi@9.2 GeV, ~ 50-100 M events for alignment, calibration and physics
- ❖ 2025 and beyond:
  - ✓ Au+Au @ 11 GeV, design luminosity
  - ✓ system size and collision energy scans

- ❖ Preparation of the MPD detector and experimental program is ongoing, all activities are continued
- ❖ All components of the MPD 1-st stage detector are in advanced state of production (subsystems, support frame, electronics platforms, LV/HV, control systems, cryogenics, cabling, etc.)

Schedule of the MPD-NICA is significantly affected by the current geopolitical situation (suspension of collaboration with CERN and Polish & Czech Republic member institutions, economical sanctions and problems with supplies of many components from western companies). The primary goal to have the MPD commissioned by the first beams at NICA collider is preserved.

Heavy-ion collisions

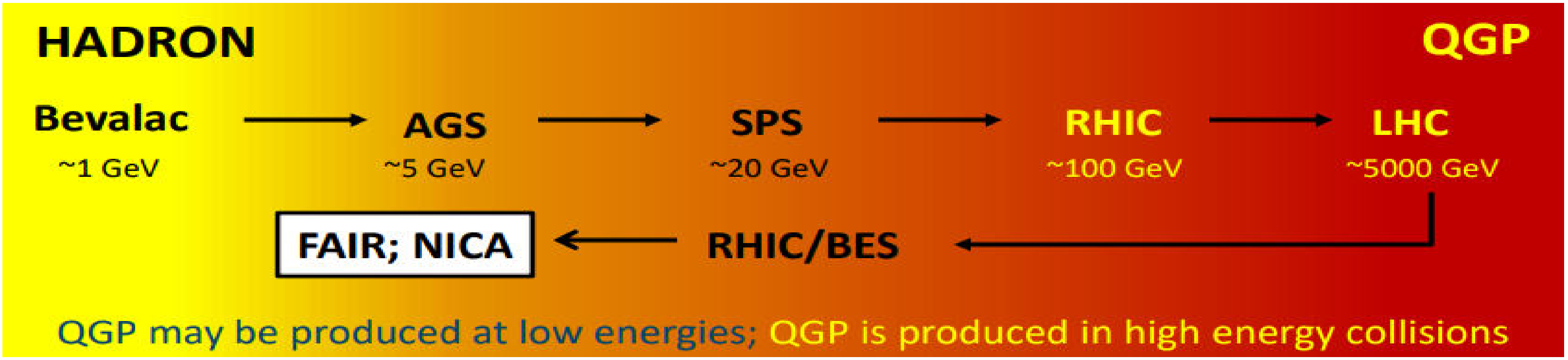

https://github.com/tgalatyuk/interaction_rate_facilities

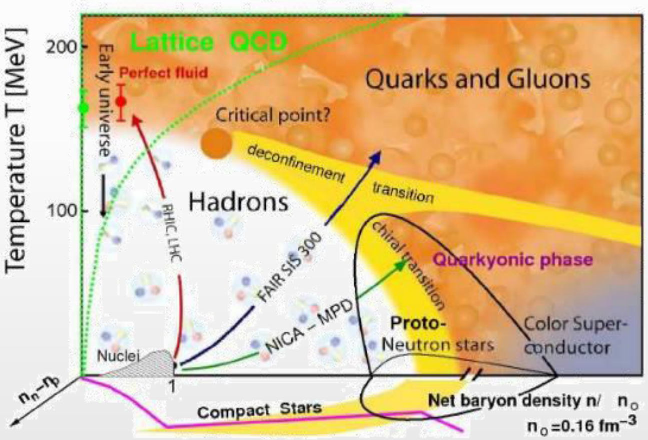

high baryon densities → inner structure of compact stars

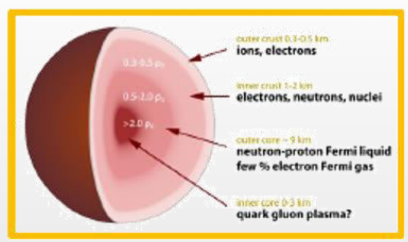

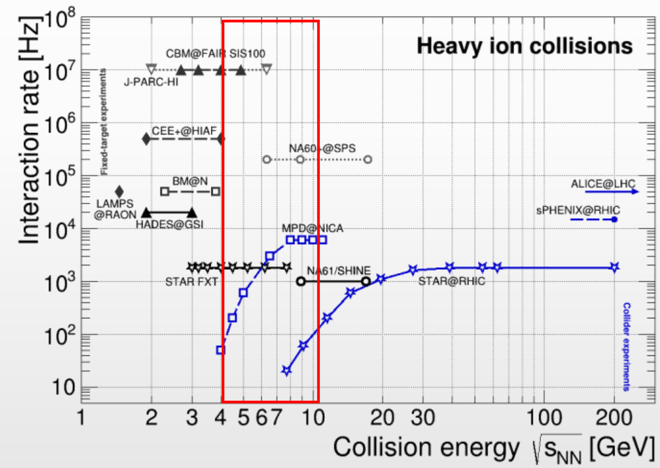

- ❖ At μ_B ~ 0, smooth crossover (lattice QCD calculations + data)
- ❖ At large μ_B, 1st order phase transition is expected → QCD critical point
- ❖ At NICA, both BM@N and MPD study QCD medium at extreme net baryon densities
- ❖ Many ongoing (HADES, NA61/Shine, STAR-BES) and future experiments in ~ same energy range

Positioning of the NICA

- Many experiments to study a similar physics case in the same decade

	NA61/SHINE at SPS	CBM at FAIR	STAR BES+FXT at RHIC	MPD + BM@N at NICA
Coverage of region of transition from baryon to meson dominance („horn”)	only higher $\sqrt{s_{NN}}$	only lower $\sqrt{s_{NN}}$	Yes (mixing collider and fixed target)	Yes (consistent acceptance)
expected luminosity (w.r.t. MPD)	lower	higher	lower	reference
possibility for system size scan	yes	yes	yes (?)	yes
full centrality range	no	yes (?)	yes	yes
acceptance type	Fixed target	Fixed target	Collider + fixed target	Collider + fixed target
running plan (heavy-ions)	approved for 2021 (per-year decision)	beyond 2025	running concluded in 2021	2023 and beyond
status at the facility (possible running time)	in competition with many projects (LHC)	CBM one of four main experiments	end of datataking (heavy-ion) in 2021	flagship experiments several months/year

- MPD strategy – high-luminosity scans in **energy** and **system size**, looking for a wide variety of signals sensitive to the phase transition and presence of the critical point
- Scans to be carried out using the **same apparatus** with all the advantages of collider experiments
  - ✓ maximum phase space, minimally biased acceptance, free of target parasitic effects

Multi-Purpose Detector (MPD) Collaboration

MPD** International Collaboration was established in **2018
to construct, commission and operate the detector

10** Countries, **>450** participants, **31** Institutes and **JINR

Organization

Acting Spokesperson:	***Victor Riabov***
Deputy Spokesperson:	***Zebo Tang***
Institutional Board Chair:	***Alejandro Ayala***
Project Manager:	***Slava Golovatyuk***

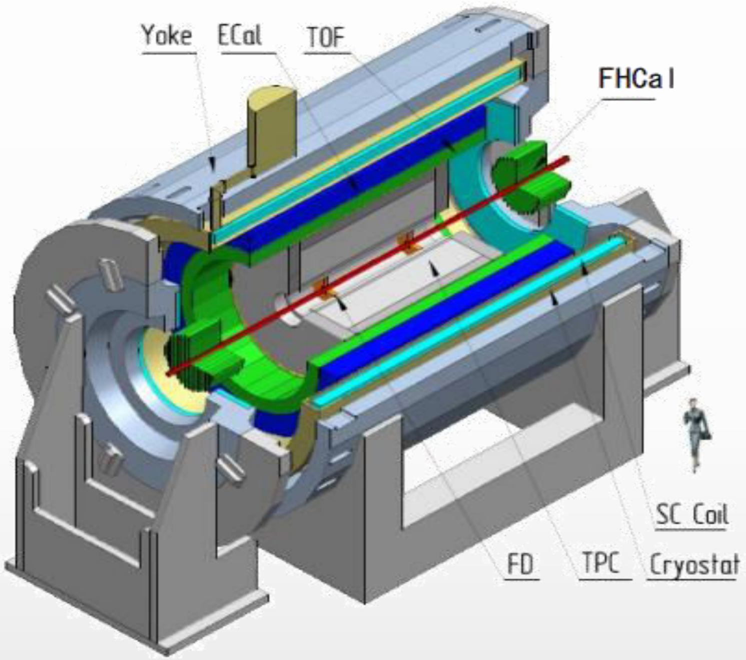

***Joint Institute for Nuclear Research**;*
*AANL, Yerevan, **Armenia;***
*University of Plovdiv, **Bulgaria;***
*Tsinghua University, Beijing, **China**;*
*USTC, Hefei, **China**;*
*Huzhou University, Huizhou, **China**;*
*Institute of Nuclear and Applied Physics, CAS, Shanghai, **China**;*
*Central China Normal University, **China**;*
*Shandong University, Shandong, **China**;*
*IHEP, Beijing, **China**;*
*University of South China, **China**;*
*Three Gorges University, **China**;*
*Institute of Modern Physics of CAS, Lanzhou, **China**;*
*Tbilisi State University, Tbilisi, **Georgia**;*
*FCFM-BUAP (Heber Zepeda) Puebla, **Mexico**;*
*FC-UCOL (Maria Elena Tejeda), Colima, **Mexico**;*
*FCFM-UAS (Isabel Dominguez), Culiacán, **Mexico**;*
*ICN-UNAM (Alejandro Ayala), Mexico City, **Mexico**;*
*Institute of Applied Physics, Chisinev, **Moldova**;*
*Institute of Physics and Technology, **Mongolia**;*

*Belgorod National Research University, **Russia**;*
*INR RAS, Moscow, **Russia**;*
*MEPhI, Moscow, **Russia**;*
*Moscow Institute of Science and Technology, **Russia**;*
*North Osetian State University, **Russia**;*
*NRC Kurchatov Institute, ITEP, **Russia**;*
*Kurchatov Institute, Moscow, **Russia**;*
*St. Petersburg State University, **Russia;***
*SINP, Moscow, **Russia**;*
*PNPI, Gatchina**, Russia**;*
*Vinča Institute of Nuclear Sciences**, Serbia**;*
*Pavol Jozef Šafárik University, Košice, **Slovakia***

MPD physics program

G. Feofilov, A. Aparin

Global observables

- Total event multiplicity
- Total event energy
- Centrality determination
- Total cross-section measurement
- Event plane measurement at all rapidities
- Spectator measurement

V. Kolesnikov, Xianglei Zhu

Spectra of light flavor and hypernuclei

- Light flavor spectra
- Hyperons and hypernuclei
- Total particle yields and yield ratios
- Kinematic and chemical properties of the event
- Mapping QCD Phase Diag.

K. Mikhailov, A. Taranenko

Correlations and Fluctuations

- Collective flow for hadrons
- Vorticity, Λ polarization
- E-by-E fluctuation of multiplicity, momentum and conserved quantities
- Femtoscopy
- Forward-Backward corr.
- Jet-like correlations

V. Riabov, Chi Yang

Electromagnetic probes

- Electromagnetic calorimeter meas.
- Photons in ECAL and central barrel
- Low mass dilepton spectra in-medium modification of resonances and intermediate mass region

Wangmei Zha, A. Zinchenko

Heavy flavor

- Study of open charm production
- Charmonium with ECAL and central barrel
- Charmed meson through secondary vertices in ITS and HF electrons
- Explore production at charm threshold

Physics capability studies using centralized Monte Carlo productions:

✓ most advanced event generators
✓ most up-to-date performance of detector subsystems
✓ common detector performance, same event/detector environment for all studies
✓ consistent picture for year-1 running with BiBi@9.2 → second collaboration paper

Collaboration activity

- Many ongoing construction works, theoretical and physics feasibility studies
- MPD publications: over 200 in total for hardware, software and physics studies:
  - ✓ RFBR grant program (now completed) attracted many new Russian institutions in the NICA activities
  - ✓ financial support for participation of Russian institutions in the MPD-NICA is needed for success of the project
- Presented at all major conferences in the field
- First collaboration paper recently published EPJA (~ 50 pages):
  - ✓ Status and initial physics performance studies of the MPD experiment at NICA, Eur.Phys.J.A 58 (2022) 7, 140

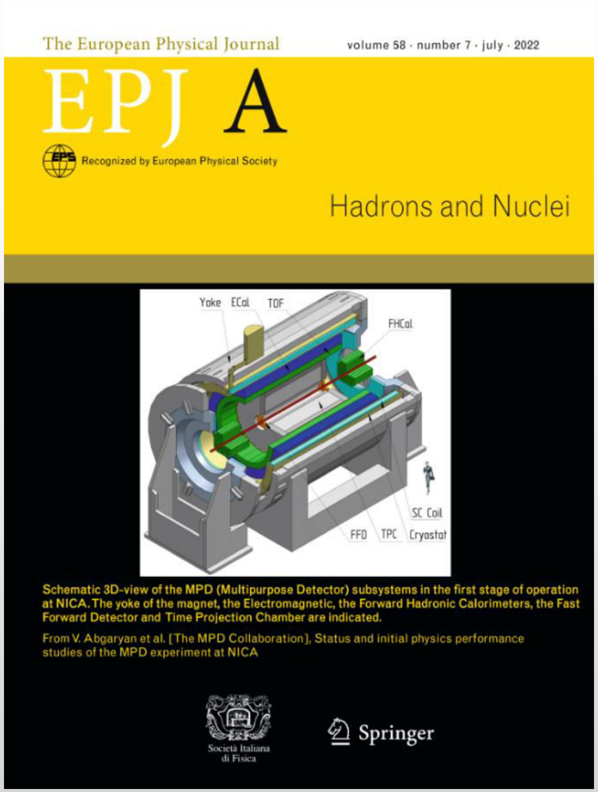

Identified light hadrons

- Probe freeze-out conditions, collective expansion, hadronization mechanisms, strangeness production ("horn" for K/π), parton energy loss, etc. with particles of different masses, quark contents/counts
- Charged hadrons: large and uniform acceptance + excellent PID capabilities of TPC and TOF

0-5% central AuAu@9 GeV (PHSD), 5 M events → full event/detector simulation and reconstruction

Phys.Part.Nucl. 53 (2022) 2, 203-206

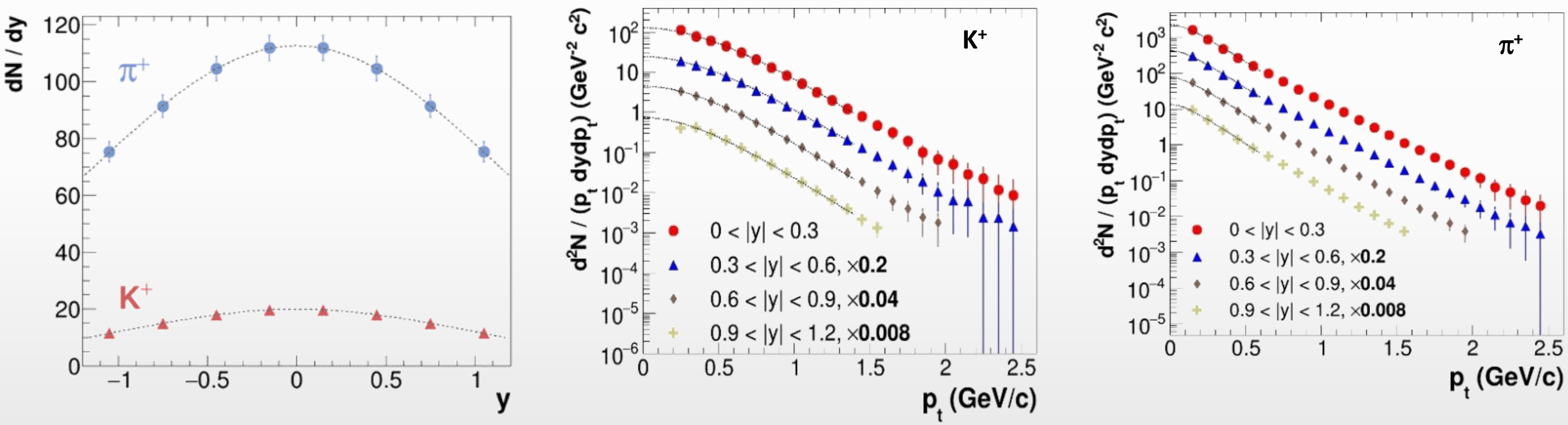

✓ sample ~ 70% of the π/K/p production in the full phase space
✓ hadron spectra are measured from p_T ~ 0.1 GeV/c

Identified light hadrons

- Neutral mesons (π^0, η, K_s, ω, η'): ECAL reconstruction + photon conversion method (PCM)

AuAu@11 GeV (UrQMD), 10M events → full event/detector simulation and reconstruction

$\pi^0 \to \gamma (\gamma \to e^+e^-) + \gamma (\gamma \to e^+e^-)$

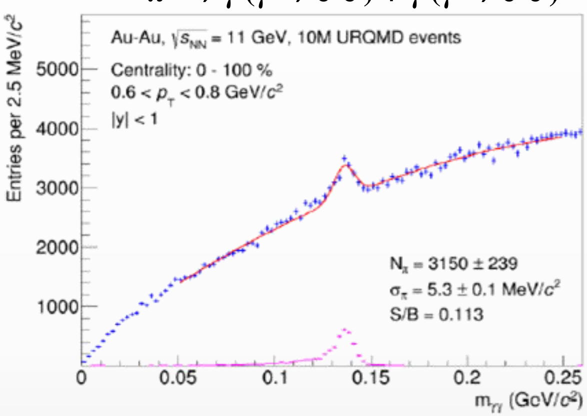

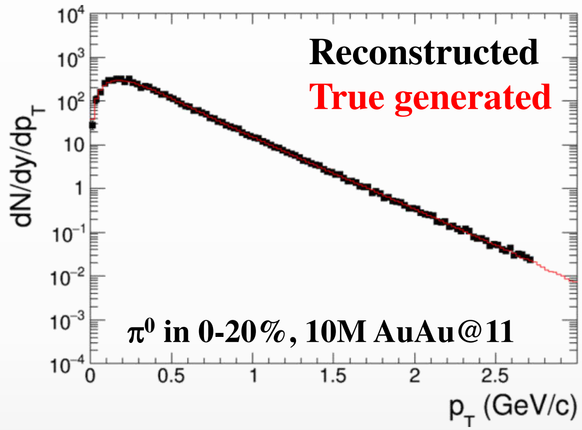

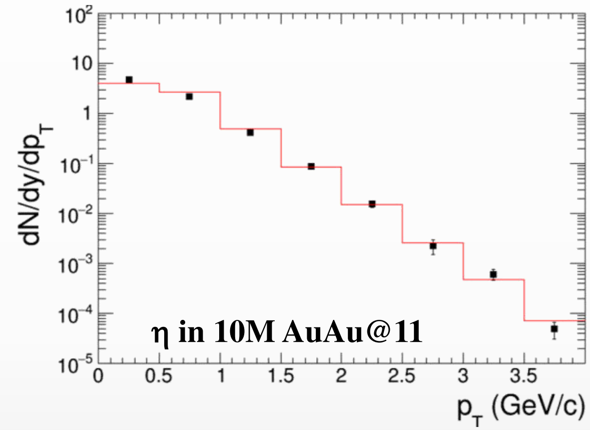

✓ extend p_T ranges of charged particle measurements
✓ different systematics

MPD will be able to measure differential production spectra, integrated yields and $\langle p_T \rangle$, particle ratios for a wide variety of identified hadrons (π, K, η, ω, p, η')

First measurements will be possible with a few million sampled heavy-ion events

Strange baryons

- Since the mid 80s, strangeness enhancement is considered as a signature of the QGP formation
- Experimentally observed in heavy-ion collisions at AGS, SPS, RHIC, and LHC energies.

NA57 and WA97 at SPS

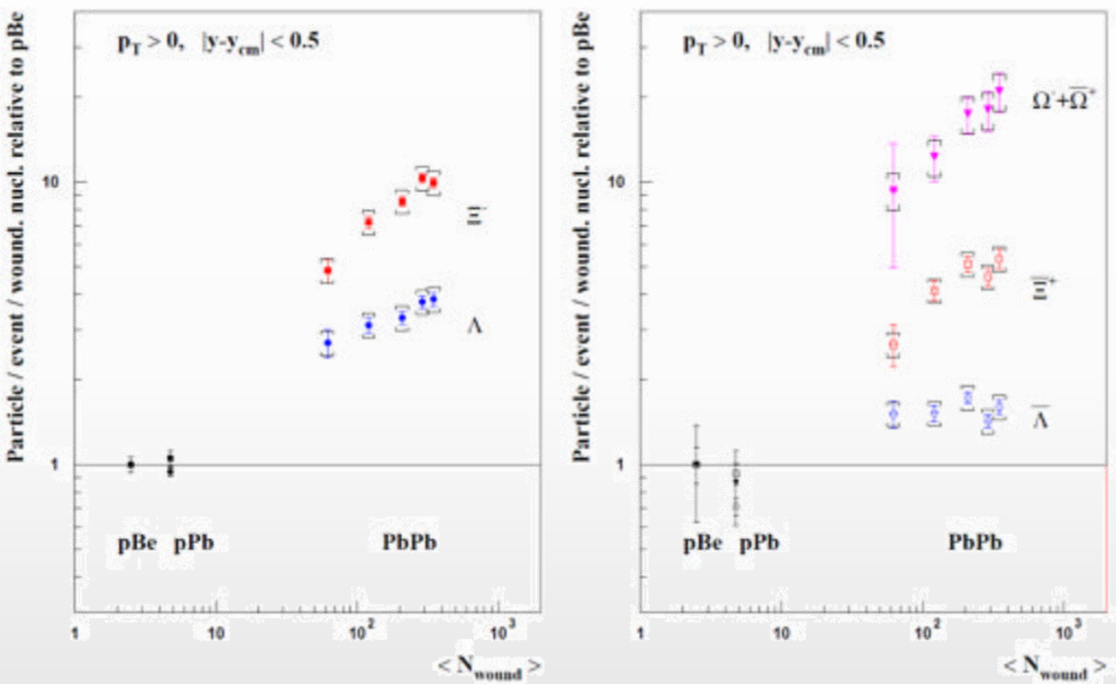

RHIC/LHC

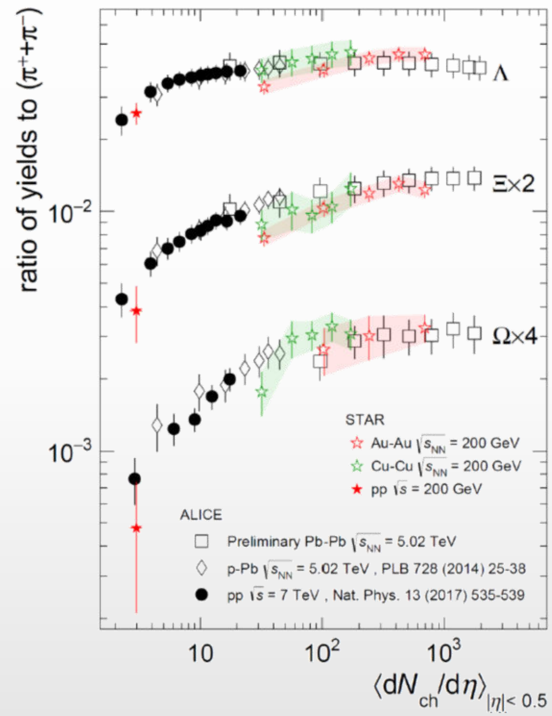

- No consensus on the dominant strangeness enhancement mechanisms:
  - ✓ strangeness enhancement in QGP contradicts with the observed collision energy dependence
  - ✓ strangeness suppression in pp within canonical suppression models reproduces most of results except for φ(1020)
- Differential measurements (vs. p_T, multiplicity, event shape, energy balance) of strange baryons are needed in different collision systems (pp, pA, AA) at NICA energies

Reconstruction of strange baryons

AuAu@11 GeV (PHSD), 10 M events → full event/detector simulation and reconstruction

Acta Physica Polonica B 14 (2021) 3, 529-532

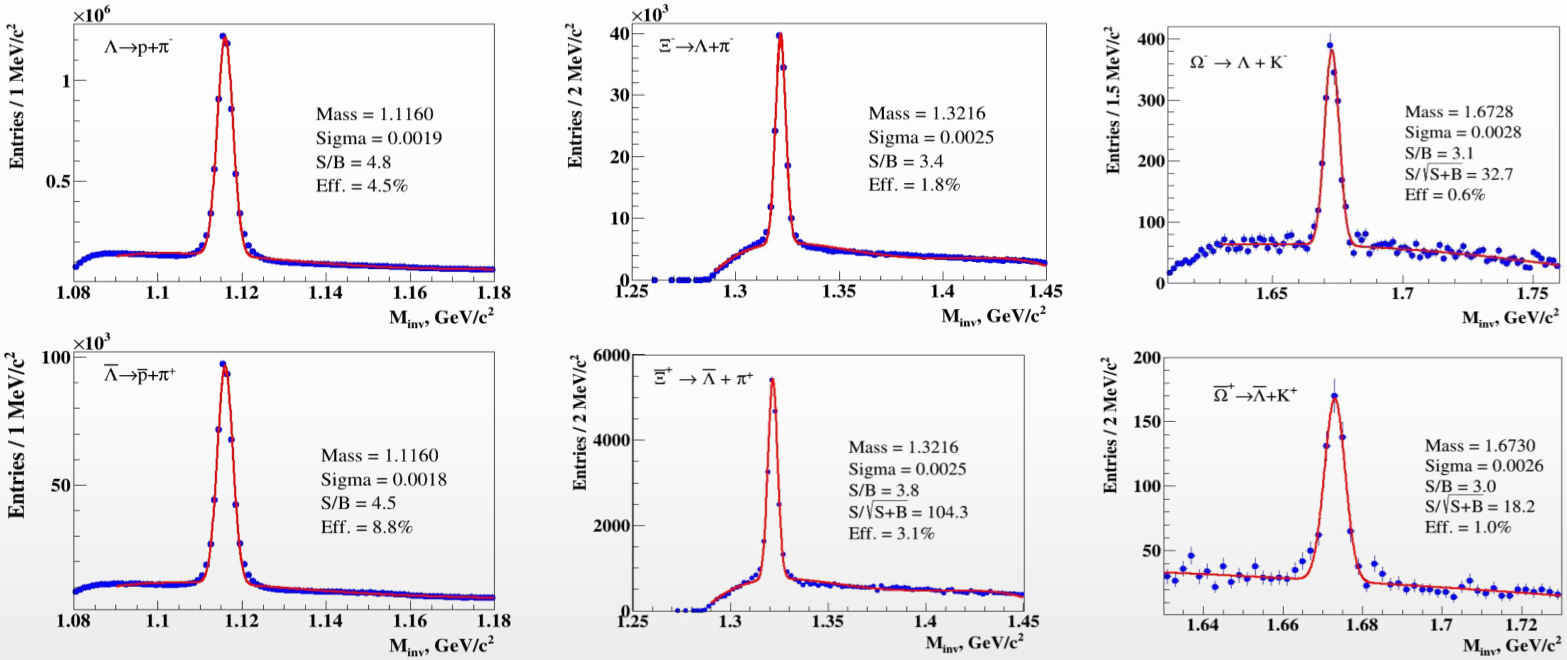

- ❖ Strange baryons can be reconstructed with good S/B ratios using charged hadron identification in the TPC&TOF and different decay topology selections

Measurement of strange baryons

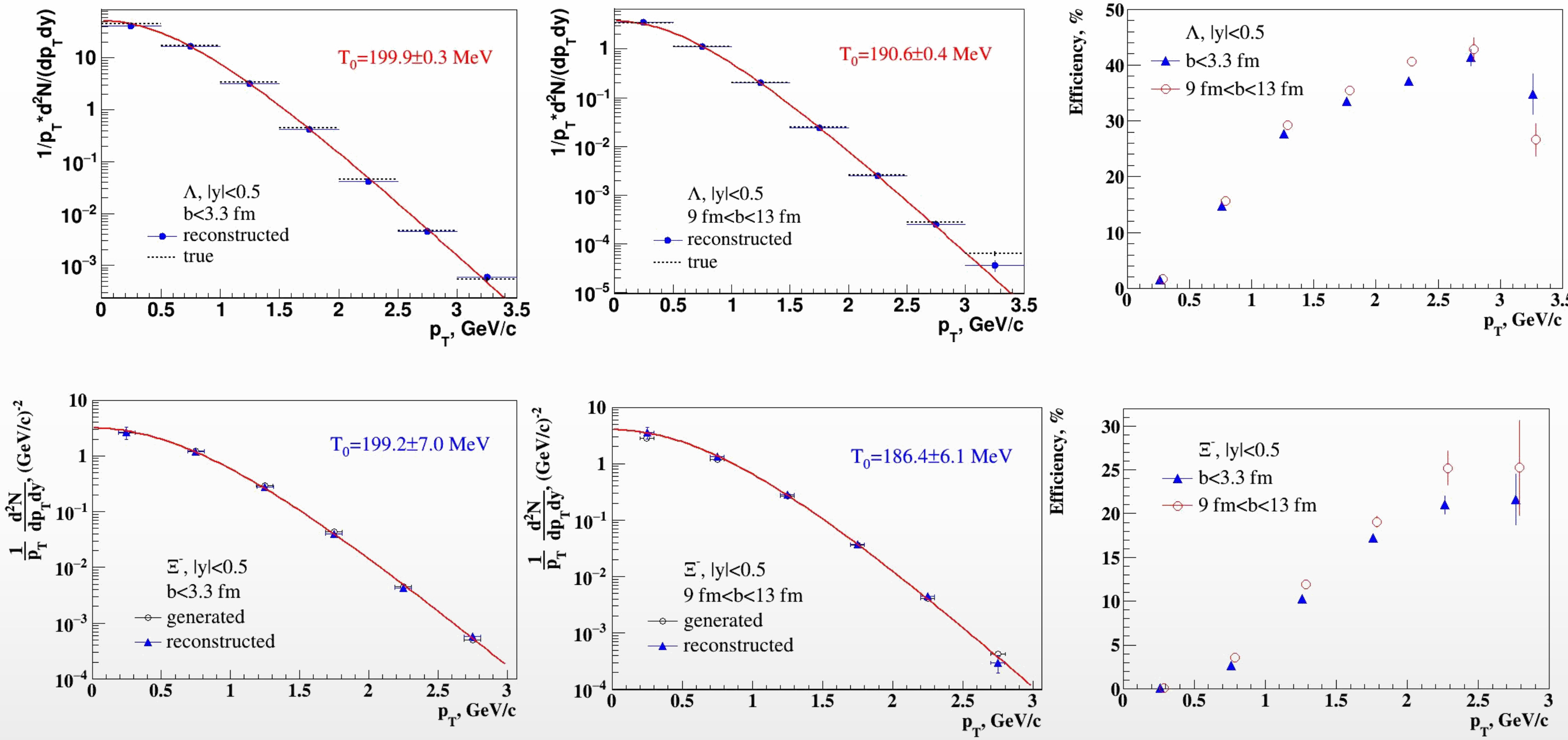

- ❖ Reconstructed spectra are consistent with the generated ones → capability to reconstruct baryon yields down to low momenta with reasonable efficiencies
- ❖ Measurements for strange baryons will be possible with accumulation of ~ 10 M BiBi@9.2 events

Hypernuclei

- Hyper nuclei measurement studies are crucial:
  - ✓ microscopic production mechanism, Y-N potential, strange sector of nuclear EoS
  - ✓ strong implications for astronuclear physics → hyperons expected to exist in the inner core of neutron stars
- Production mechanism usually described with two classes of phenomenological models :
  - ✓ statistical hadronization (SHM) → production during phase transition, $dN/dy \propto \exp(-m/T_{chem})$ [1]
  - ✓ coalescence → (anti)nucleons close in phase space ($\Delta p < p_0$) and matching the spin state form a nucleus [2]
- Models predict enhanced hypernuclear production at NICA→ double hypernuclei are reachable

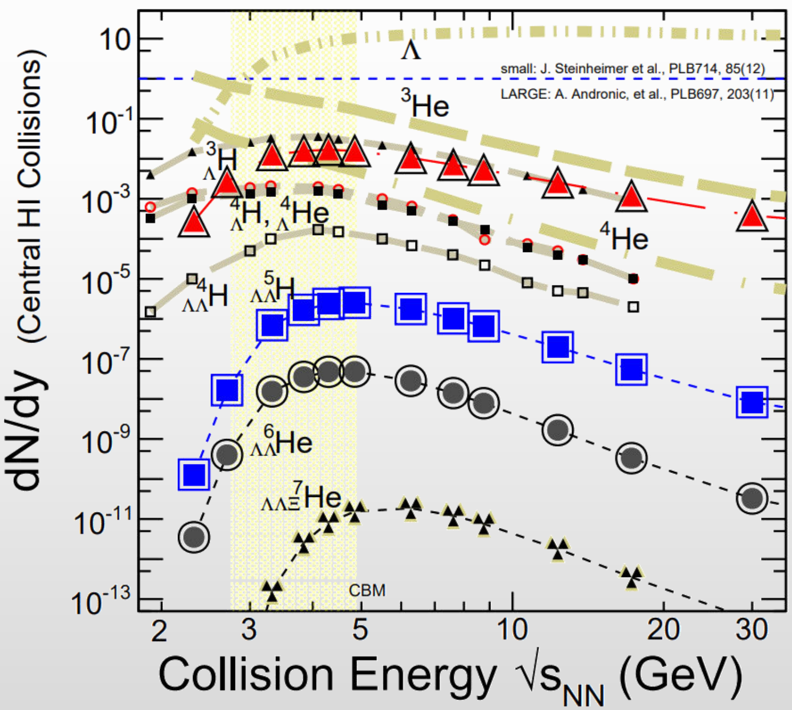

- Reconstruction of hypernuclei requires detection and identification of light nuclei and precise secondary vertex reconstruction:

$$^{3}_{\Lambda}H \rightarrow {}^{3}He + \pi^-$$
$$^{3}_{\Lambda}H \rightarrow d + p + \pi^-$$
$$^{4}_{\Lambda}H \rightarrow {}^{4}He + \pi^-$$
$$^{4}_{\Lambda}He \rightarrow {}^{3}He + p + \pi^-$$

- Observables of interest: precise measurements of binding energies, lifetimes and branching ratios

[1] Andronic et al., Nature 561 (2018) 321–330
[2] Butler et al., Phys. Rev. 129 (1963) 836

Reconstruction of hypertritons

BiBi@9.2 GeV (PHQMD), 40 M events → full event/detector simulation and reconstruction

Phys.Part.Nucl.Lett. 19 (2022) 1, 46-53

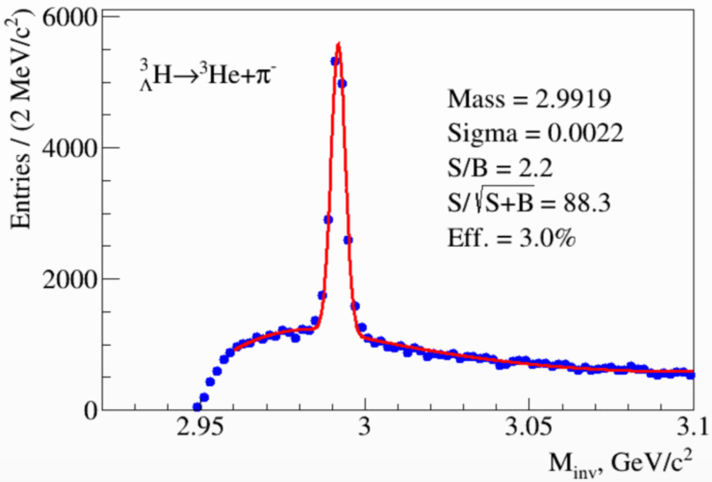

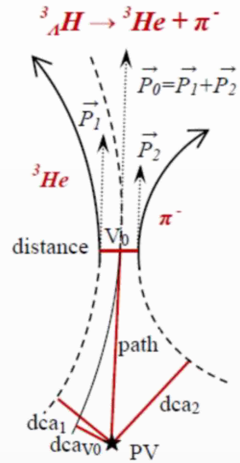

Decay channel	Branching ratio	Decay channel	Branching ratio
$\pi^{-} + {}^{3}He$	24.7%	$\pi^{-} + p + p + n$	1.5%
$\pi^{0} + {}^{3}H$	12.4%	$\pi^{0} + n + n + p$	0.8%
$\pi^{-} + p + d$	36.7%	$d + n$	0.2%
$\pi^{0} + n + d$	18.4%	$p + n + n$	1.5%

Spectrum is reconstructed up to p_T=4.5 GeV/c

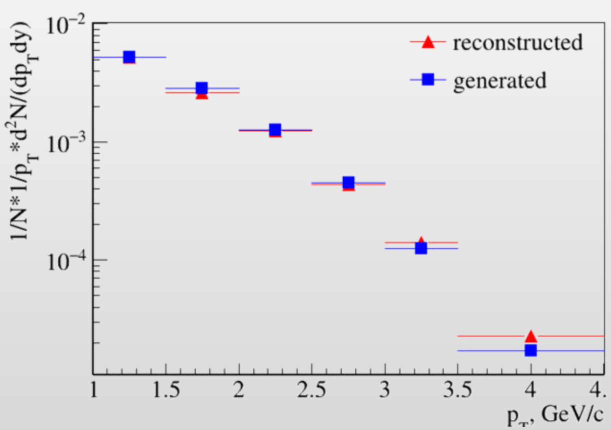

$$N(\tau) = N(0)\exp\left(-\frac{\tau}{\tau_0}\right) = N(0)\exp\left(-\frac{ML}{cp\tau_0}\right),$$

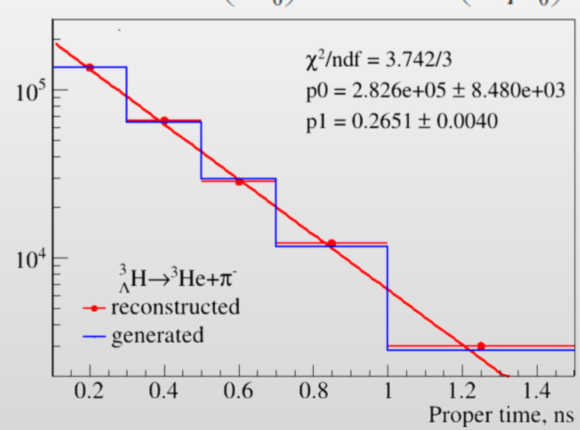

❖ First measurements for hypertriton will be possible with accumulation of ~ 50 M BiBi@9.2 events

Heavier hypernuclei

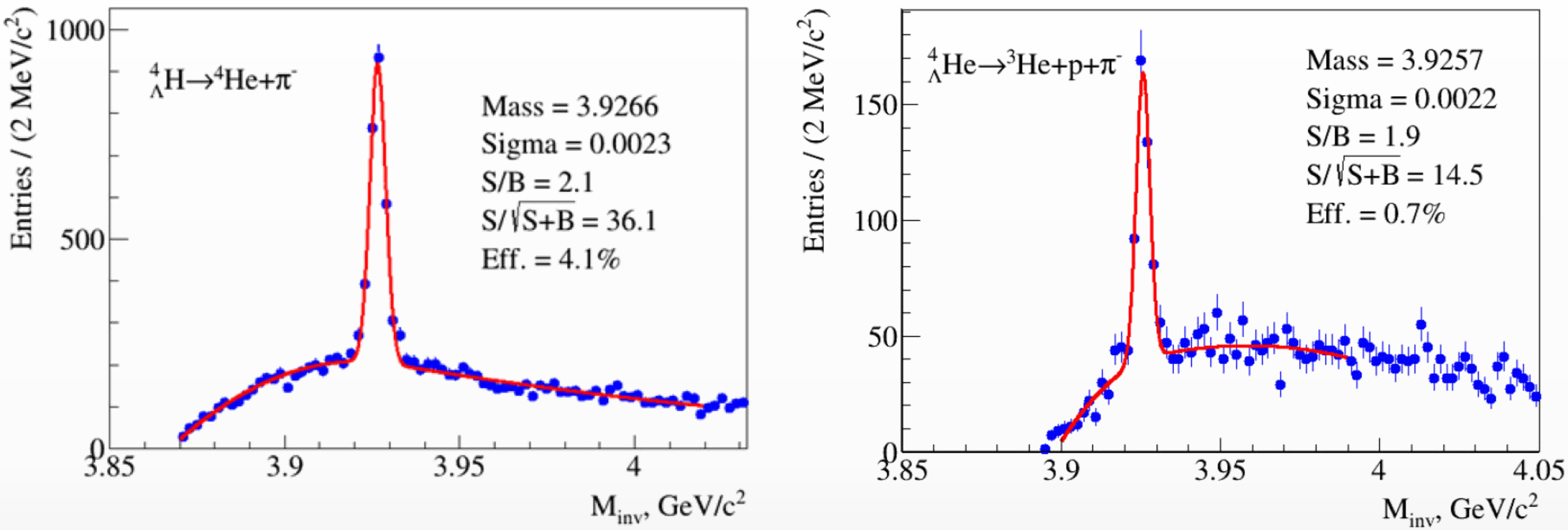

- ❖ Monte Carlo events enriched with hypernuclei distributed by (η-p_T) phase space predicted by PHQMD
- ❖ Signals for heavier hypernuclei can be reconstructed with the equivalent statistics of ~140 M events

Critical fluctuations

- Ratio of the 4th-to2nd moment of the (net)proton multiplicity distribution:
  - ✓ non-monotonic behavior → deviation from non-critical dynamic baseline close to CEP ???
  - ✓ need significant improvement of statistical precision and systematic uncertainties + extra points in the NICA energy range

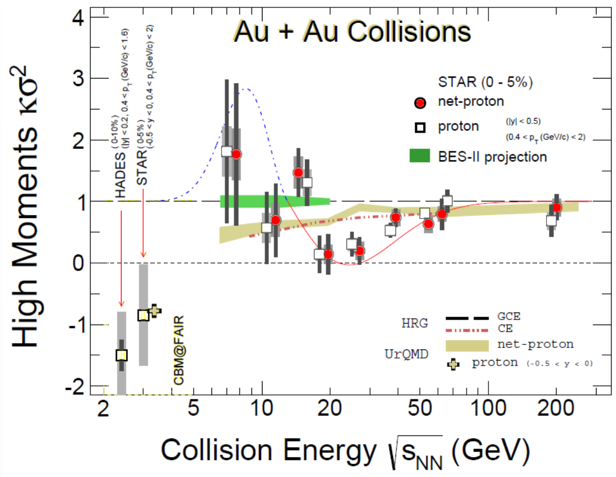

AuAu@11 (UrQMD), 5-50·10⁴ events→ full event/detector simulation and reconstruction

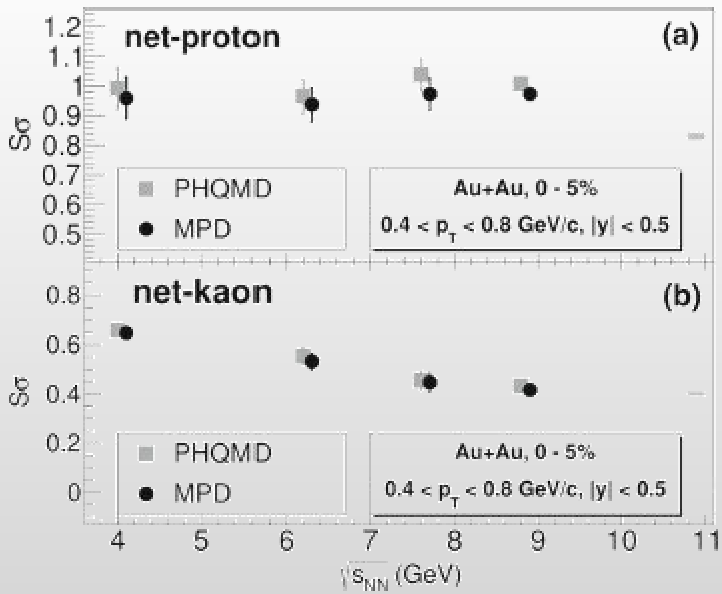

Effective skewness Sσ for net-protons (a) and net-kaons (b) in Au+Au interactions at several collision energies are reproduced

Global hyperon polarization

- Large angular momentum and strong magnetic field formed in mid-central heavy-ion collisions → polarization of particles in the final state

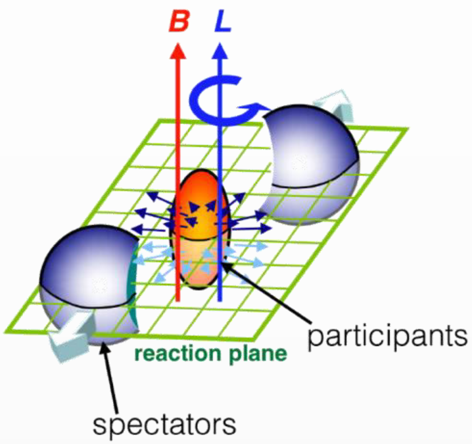

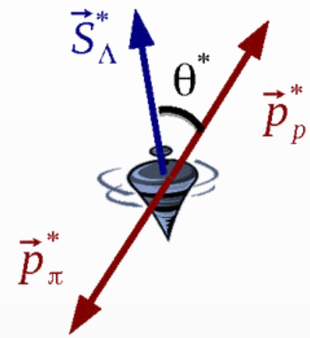

- $\Lambda/\bar{\Lambda}$ are "self-analyzing" probes → preferential emission of proton in in spin direction

STAR, Nature 548, 62 (2017)

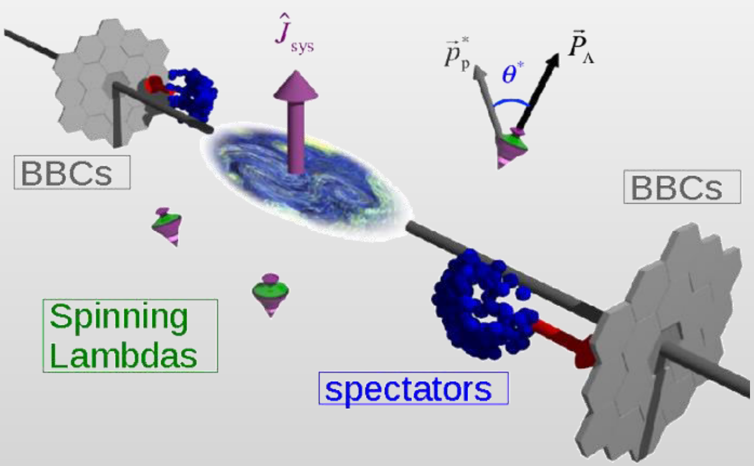

Phys.Rev.Lett.94:102301,2005;
Erratum-ibid.Lett.96:039901,2006

The global polarization observable is defined by [34]:

$$P_\Lambda = \frac{8}{\pi\alpha_\Lambda}\frac{\langle\sin(\Psi_{EP} - \phi^*_p)\rangle}{R_{EP}}. \quad (1)$$

Here $\alpha_\Lambda = 0.732 \pm 0.014$ [35] is the Λ decay parameter, Ψ_{EP} the event plane angle, ϕ^*_p the azimuthal angle of the proton in the Λ rest frame, R_{EP} the resolution of the event plane angle and the brackets $\langle.\rangle$ denote the average

Global hyperon polarization

- Global hyperon polarization measurements in mid-central A+A collisions at $\sqrt{s_{NN}}$= 3-5000 GeV

STAR, Phys.Rev.C, 104(6):L061901, 2021

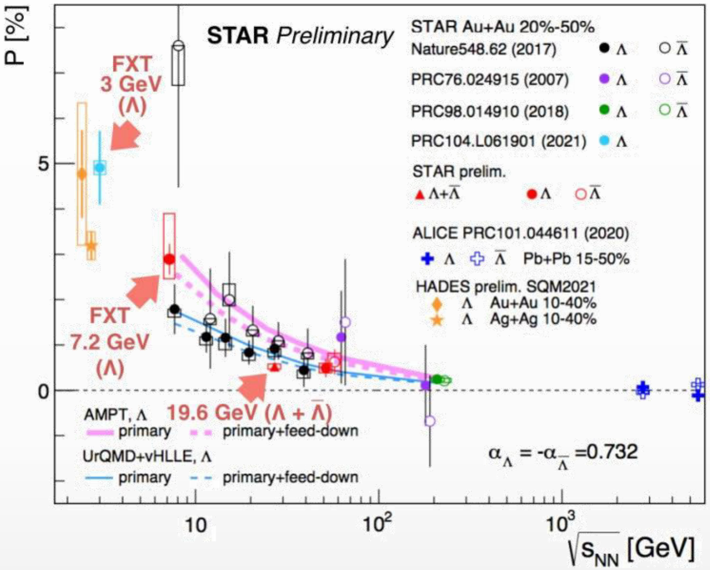

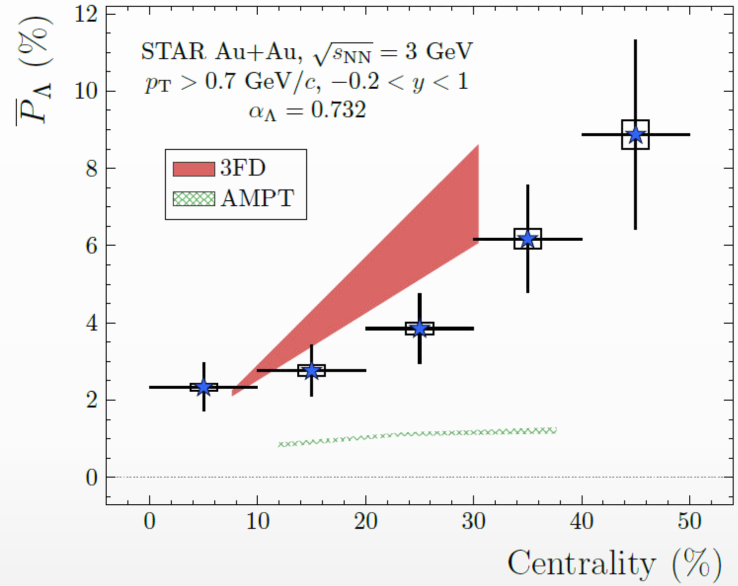

- Global polarization of hyperons experimentally observed, decreases with $\sqrt{s_{NN}}$
- Hint for a Λ-$\bar{\Lambda}$ difference, magnetic field, $P_\Lambda \simeq \frac{1}{2}\frac{\omega}{T} + \frac{\mu_\Lambda B}{T}$, $P_{\bar{\Lambda}} \simeq \frac{1}{2}\frac{\omega}{T} - \frac{\mu_\Lambda B}{T}$?
- Feed down from Σ(1385) → Λπ, Σ^0 →Λγ; Ξ→Λπ reduces polarization by ~ 10-20%
- Energy dependence of global polarization is reproduced by AMPT, 3FD, UrQMD+vHLLE
- AMPT with partonic transport strongly underestimates measurements at $\sqrt{s_{NN}}$ = 3 GeV → hadron gas?

MPD: extra points in the energy range 3-10 10 GeV with small uncertainties; centrality, p_T and rapidity dependence of polarization not only for Λ, but other (anti)hyperons (Λ, Σ, Ξ)

Measurement of global polarization

- BiBi@9.2 GeV (PHSD), ~1 M events → full event/detector simulation and reconstruction
- Global hyperon polarization (thermodynamical Becattini approach [1]) by the event generator
  → reproduce at generator level basic features measured by STAR

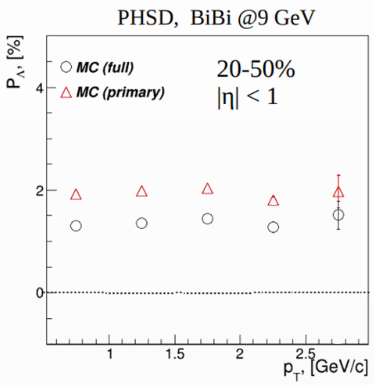

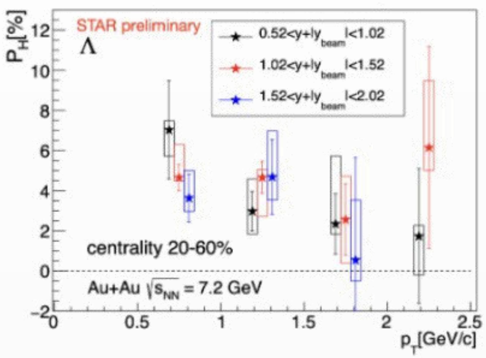

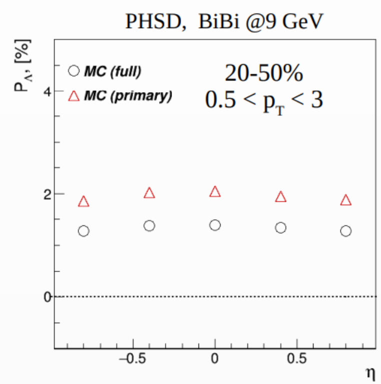

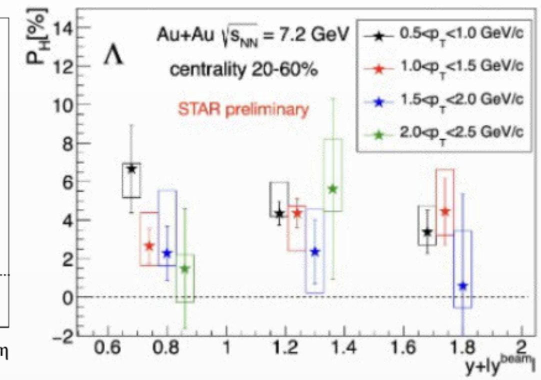

- Reconstruction of Λ global polarization with 1M sampled AuAu@9 events (work in progress):

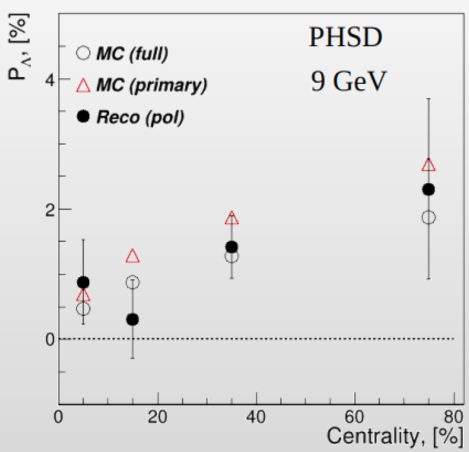

- Measured polarization is consistent with the generated one
- First global polarization measurements for $\Lambda/\bar{\Lambda}$ will be possible with ~ 10M data sampled events

[1] F. Becattini, V. Chandra, L. Del Zanna, E. Grossi, Ann. Phys. 338 (2013) 32

Anisotropic flow at RHIC/LHC

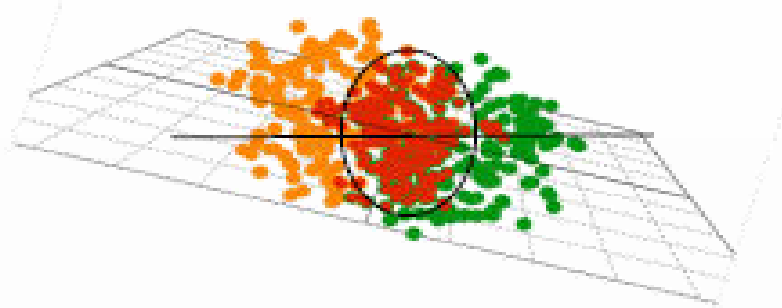

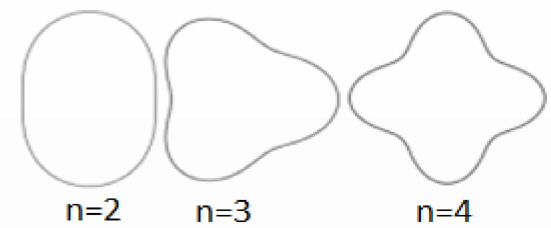

$$\epsilon_n = \sqrt{\frac{\langle r^n \cos n\phi\rangle + \langle r^n \sin n\phi\rangle}{\langle r^n\rangle}} \quad \Rightarrow \quad \frac{dN}{d\phi} \propto \left(1 + 2\sum_{n=1} v_n \cos\left[n\left(\phi - \Psi_n\right)\right]\right)$$

❖ Initial eccentricity and its fluctuations drive momentum anisotropy v_n with specific viscous modulation

Gale, Jeon et al., Phys. Rev. Lett. 110, 012302

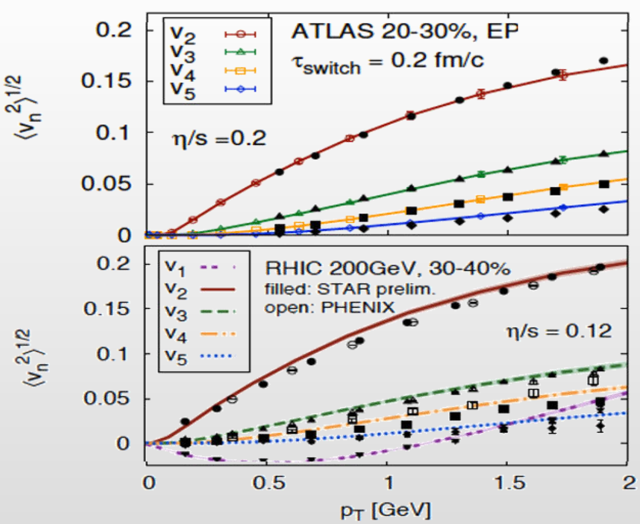

Phys. Rev. Lett. 122 (2019) 172301

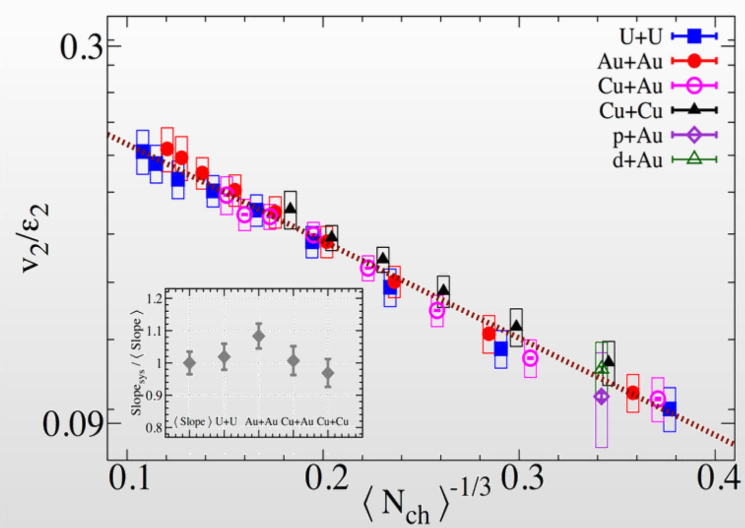

❖ Evidence for a dense perfect liquid found at RHIC/LHC [1]

[1] M. Roirdan and W. Zajc, Scientific American, May 2006

Beam energy dependence

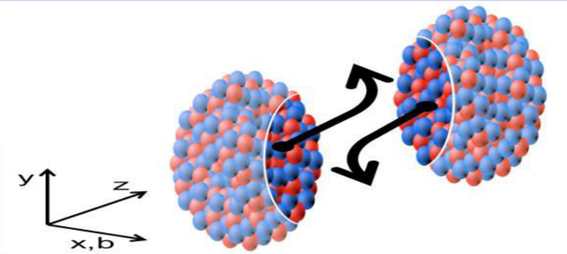

- Generated during the nuclear passage time (2R/γ) – sensitive to EOS
- RHIC @ 200 GeV (2R/γ) ~ 0.1 fm/c
- AGS @ 3-4.5 GeV (2R/γ) ~ 9-5 fm/c
- v_1 and v_2 show strong centrality, energy and species dependence

Phys.Rev.Lett. 112 (2014) 16, 162301

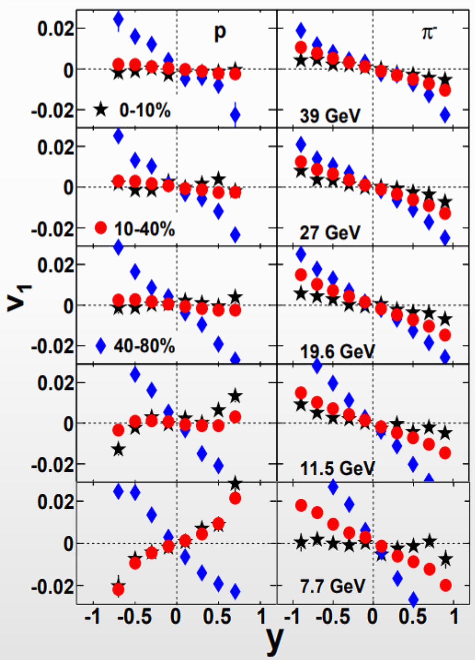

✓ models do not reproduce measurements

EPJ Web Conf. 204 (2019) 03009

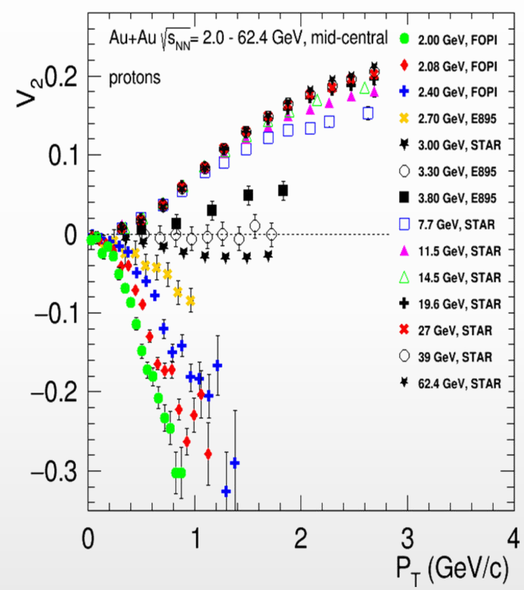

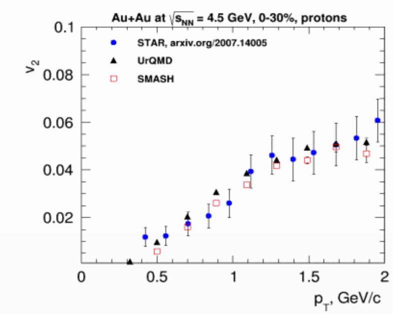

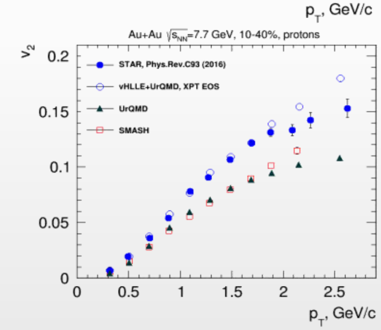

✓ $\sqrt{s_{NN}}$ ~ 3-4.5 GeV, pure hadronic models reproduce v_2 (JAM, UrQMD) → degrees of freedom are the interacting baryons

✓ $\sqrt{s_{NN}} \geq$ 7.7 GeV, need hybrid models with QGP phase (vHLLE+UrQMD, AMPT with string melting,…)

MPD: flow measurements as a function of p_T, rapidity and particle species → test of modeling approaches, microscopic degrees of freedom. Collision system scan → vary the initial condition and observe its influence for the final state

v_2 for pions and protons

AuAu@7.7 GeV (UrQMD), 15 M events → full event/detector simulation and reconstruction

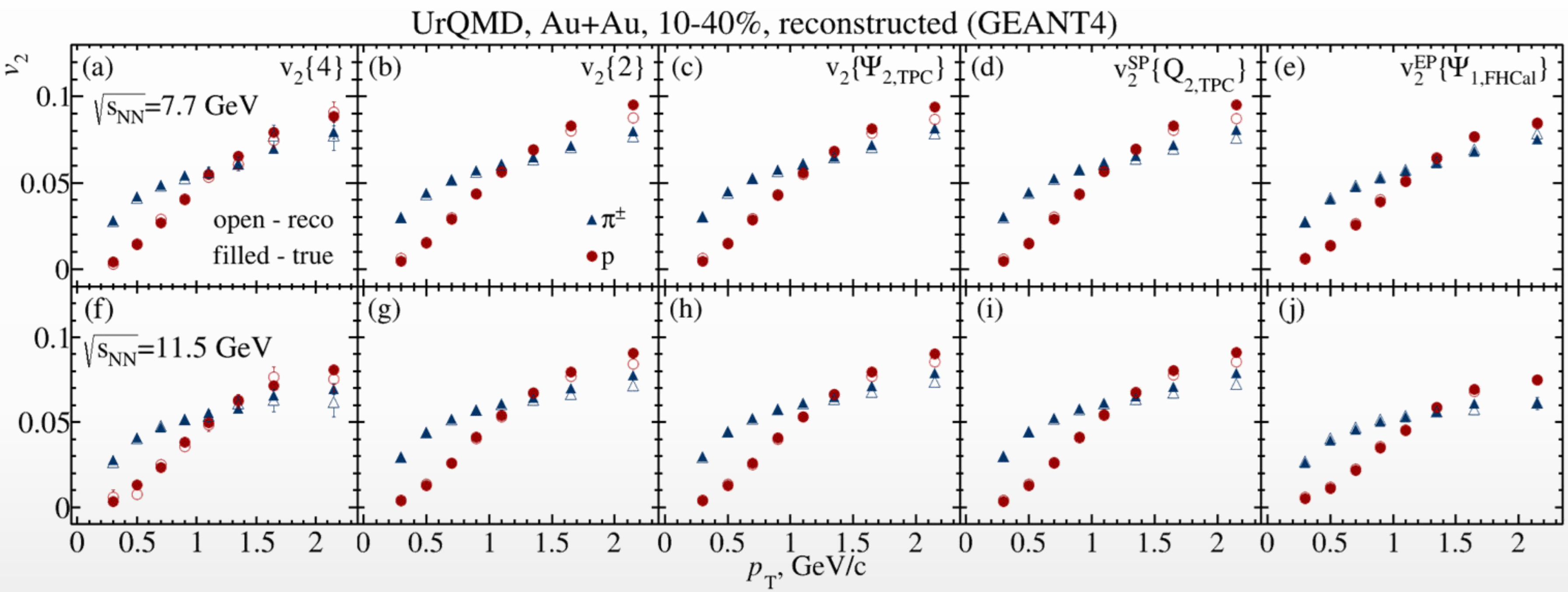

❖ Reconstructed and generated v_2 of pions and protons are in good agreement for all methods

Higher harmonics (v_3)

AuAu@11.5 GeV (vHLLE + UrQMD), 15 M events → full event/detector simulation and

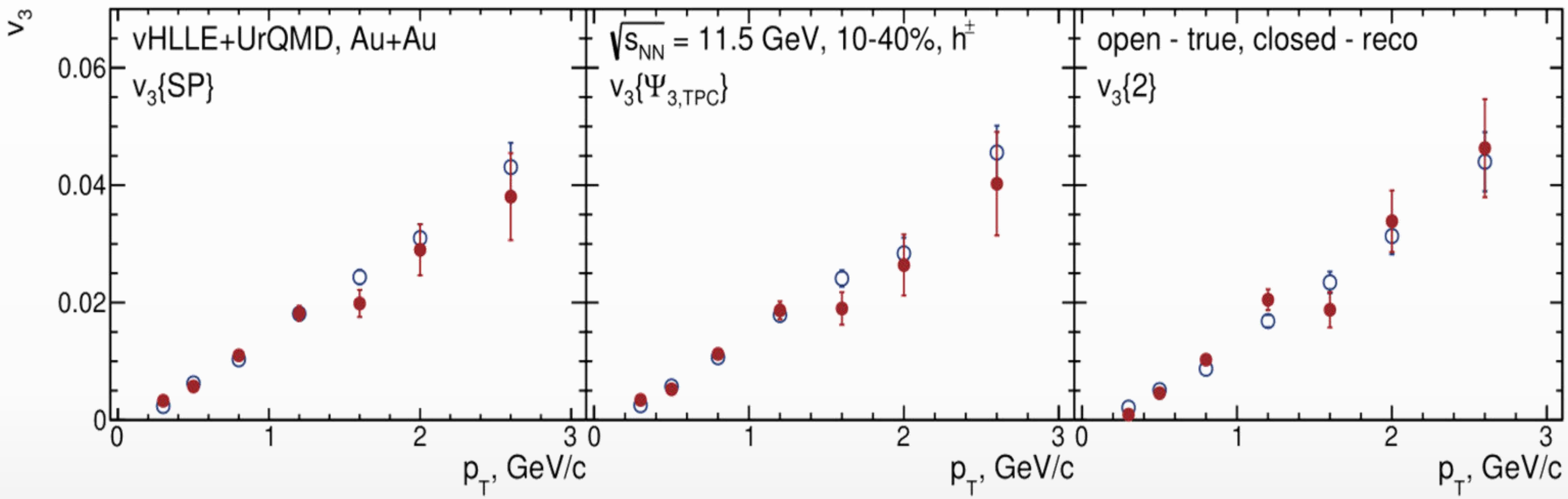

- Reconstructed and generated v_3 of charged hadrons are in good agreement for all methods
- Models show that higher harmonic ripples are more sensitive to the existence of a QGP phase

Collective flow for V0 (K_s^0 and Λ)

AuAu@11 GeV (UrQMD), 25 M events → full event/detector simulation and reconstruction

$$\nu_2^{SB}(m_{inv},p_T) = \nu_2^{S}(p_T)\frac{N^S(m_{inv},p_T)}{N^{SB}(m_{inv},p_T)} + \nu_2^{B}(m_{inv},p_T)\frac{N^B(m_{inv},p_T)}{N^{SB}(m_{inv},p_T)}$$

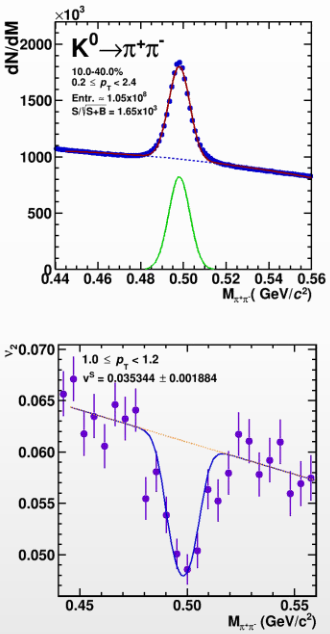

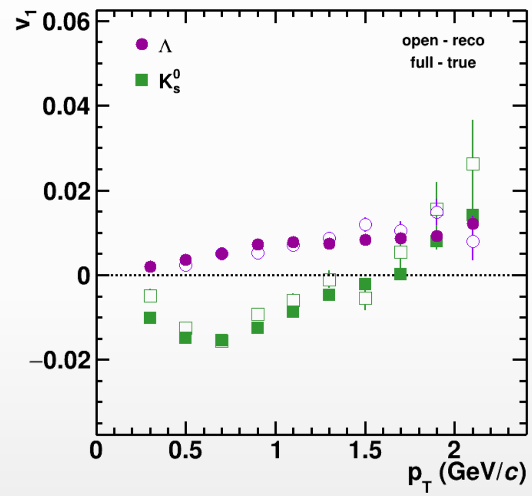

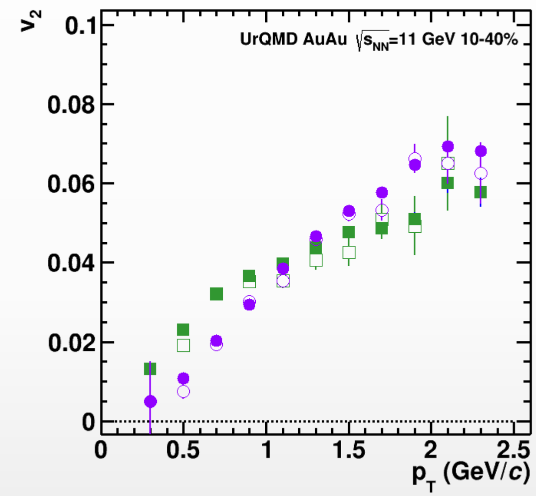

- ❖ Differential flow signal extraction using invariant mass fit method
- ❖ Reasonable agreement between reconstructed and generated v_n signals for K_S^0 and Λ

Short-lived resonances

❖ Resonances are best suited to probe density and lifetime of the late hadronic phase of HI collisions

increasing lifetime →

	ρ(770)	K*(892)	Σ(1385)	Λ(1520)	Ξ(1530)	ϕ(1020)
cτ (fm/c)	1.3	4.2	5.5	12.7	21.7	46.2
$\sigma_{rescatt}$	$\sigma_\pi \sigma_\pi$	$\sigma_\pi \sigma_K$	$\sigma_\pi \sigma_\Lambda$	$\sigma_K \sigma_p$	$\sigma_\pi \sigma_\Xi$	$\sigma_K \sigma_K$

Final state yields of resonances depend on:

resonance yields at chemical freeze-out
lifetime of the resonance and the hadronic phase
type and scattering cross sections of daughter particles

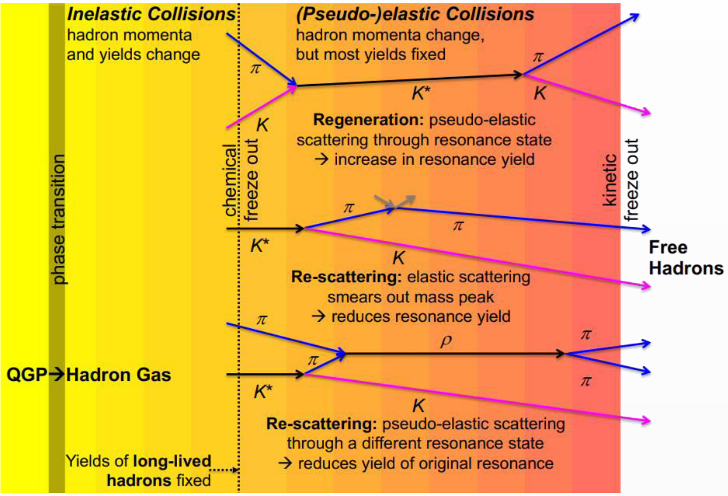

❖ Suppression of short-lived ρ^0, $K^*(892)^0$, $\Sigma(1385)^\pm$ and Λ(1520) resonances was observed in central A+A collisions at SPS, RHIC and LHC → dominance of rescattering over regeneration → consistent with existence of a long enough hadronic phase → hadronic phase lifetime ~ 10 fm/c

❖ Hadronic phase affects most of observables measured in the final state (flow, correlations, yields, etc.)

❖ Measurements for resonances are vital to cross check the hadronic phase models

❖ Only models with validated hadronic phase afterburners can be used for comparison with real data to infer properties of the early partonic phase of heavy-ion collisions

Polarization of vector mesons: $K^*(892)$ and ϕ

Non-central heavy-ion collisions:

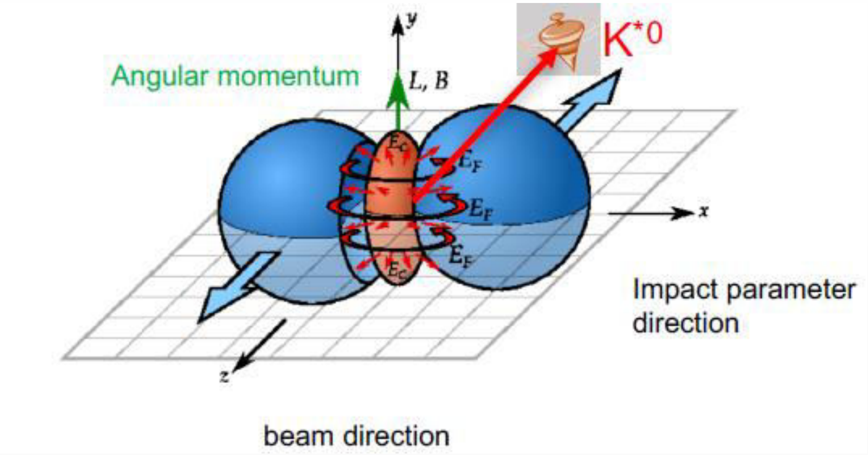

NPA 1005 (2021) 121733

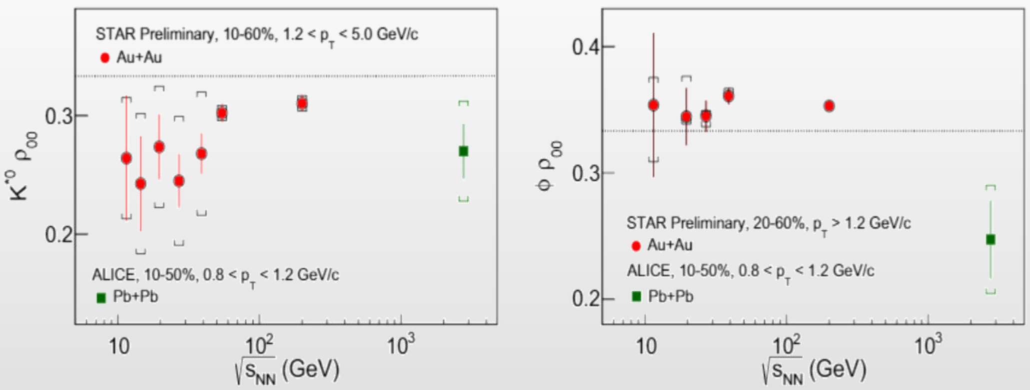

- Light quarks can be polarized by $|\bar{J}|$and $|\bar{B}|$
- If vector mesons are produced via recombination their spin may align
- Quantization axis:
  - ✓ normal to the production plane (momentum of the vector meson and the beam axis)
  - ✓ normal to the event plane (impact parameter and beam axis)
- Measured as anisotropies:

$$\frac{dN}{dcos\theta} = N_0\left[1 - \rho_{0,0} + cos^2\theta\left(3\rho_{0,0} - 1\right)\right]$$

$\rho_{0,0}$ is a probability for vector meson to be in spin state = 0 → $\rho_{0,0}$ = 1/3 corresponds to no spin alignment

- Measurements at RHIC/LHC challenge theoretical understanding → ρ_{00} can depend on multiple physics mechanisms (vorticity, magnetic field, hadronization scenarios, lifetimes and masses of the particles)

Reconstruction of resonances

BiBi@9.2 GeV (UrQMD), 10 M events→ full event/detector simulation and reconstruction

Invariant mass distributions after mixed-event background subtraction

Phys.Scripta 96 (2021) 6, 064002

$\phi(1020) \rightarrow K^+K^-$

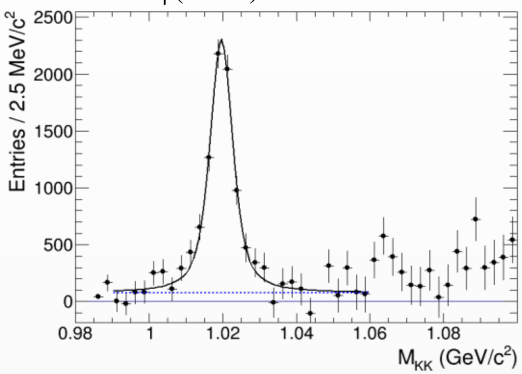

$K^*(892)^\pm \rightarrow \pi^\pm K_s$ ($K_s \rightarrow \pi^+\pi^+$)

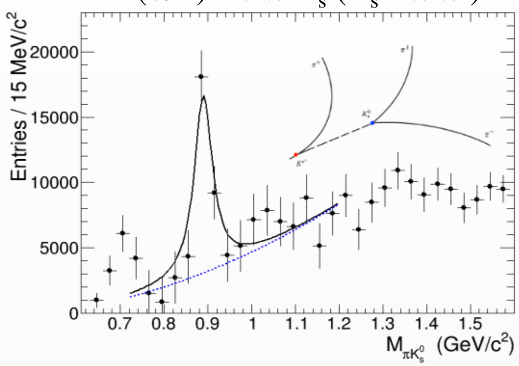

$K^*(892)^0 \rightarrow \pi^\pm K^\pm$

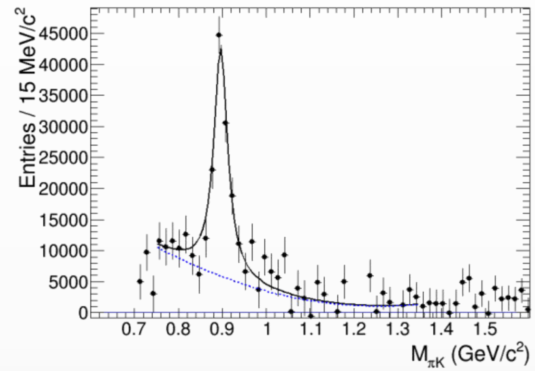

$\Sigma(1385)^\pm \rightarrow \pi^\pm\Lambda$ ($\Lambda \rightarrow p\pi$)

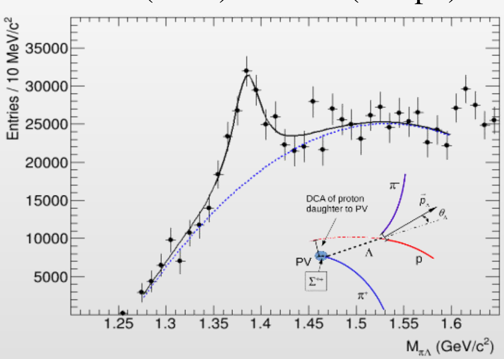

$\Lambda(1520) \rightarrow pK^-$

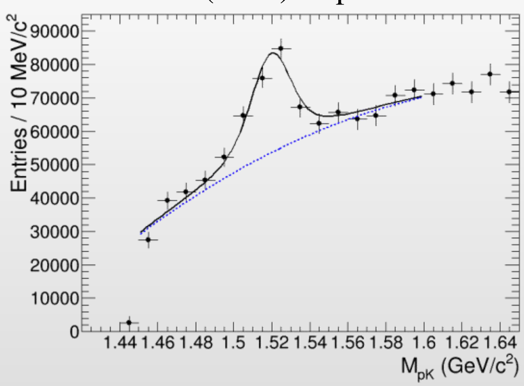

$\Xi(1530)^0 \rightarrow \pi^+\Xi^-$ ($\Xi^- \rightarrow \Lambda\pi^-$, ($\Lambda \rightarrow p\,\pi^-$))

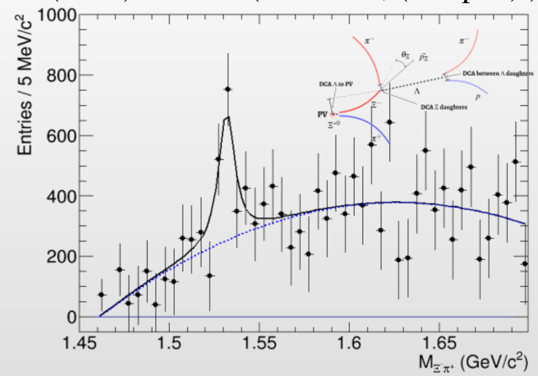

- ❖ MPD can reconstruct resonance signals using combined charged particle identification in TPC+TOF and secondary vertex topology selections for weakly decaying daughters

NICA

Measurement of resonances

BiBi@9.2 GeV (UrQMD), 10 M events→ full event/detector simulation and reconstruction

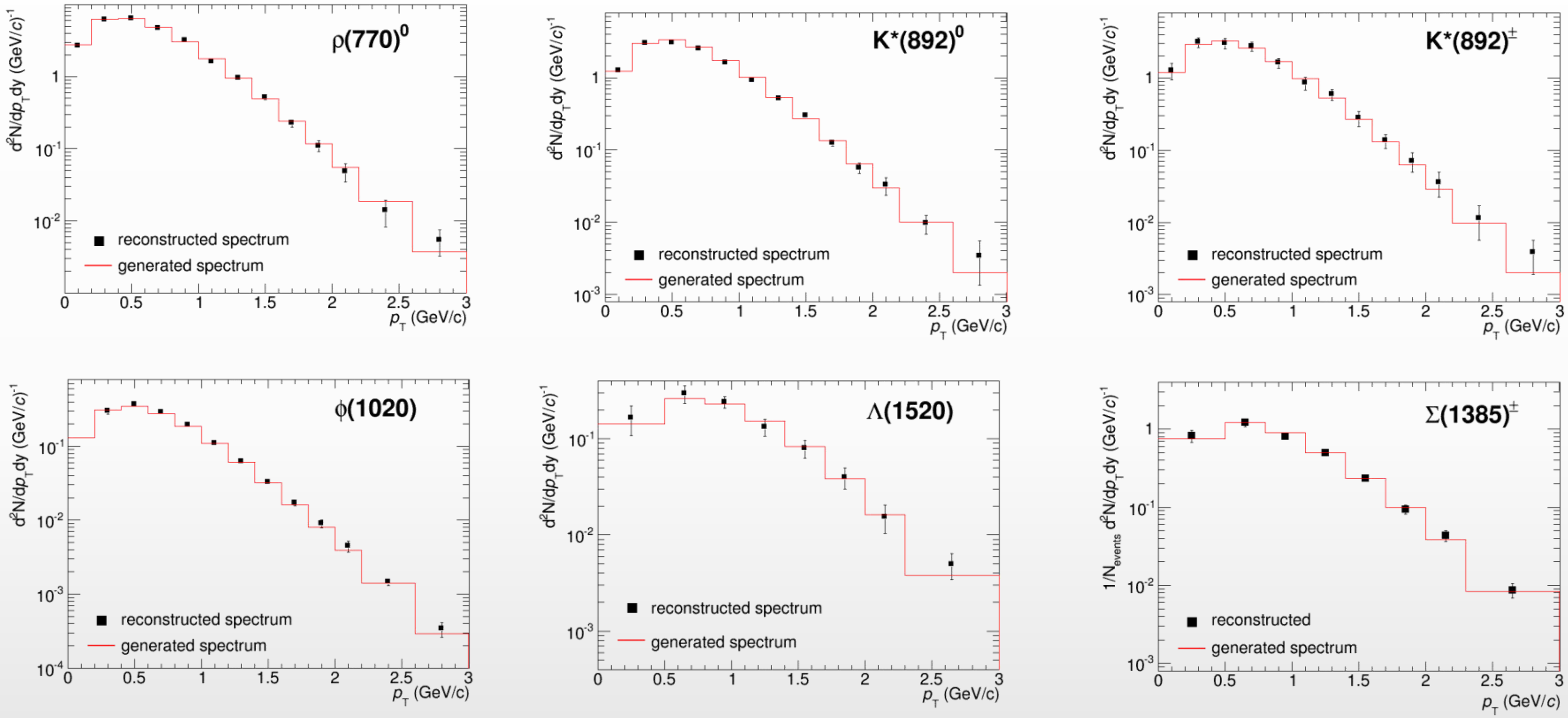

- ❖ Reconstructed spectra match the generated ones within uncertainties
- ❖ First measurements for resonances will be possible with accumulation of ~ 10 M Bi+Bi events
- ❖ Measurements are possible starting from ~ zero momentum → sample most of the yield

Other observables …

- Femtoscopy measurements:
  - ✓ size of the particle-emitting region and space-time evolution of the produced system
  - ✓ Y-N, Y-Y interaction potential (Nature 588 (2020) 7837, 232-238)
- Measurement for pions are straightforward and robust, large discovery potential in correlations for kaons and protons, as well as correlations including hyperons

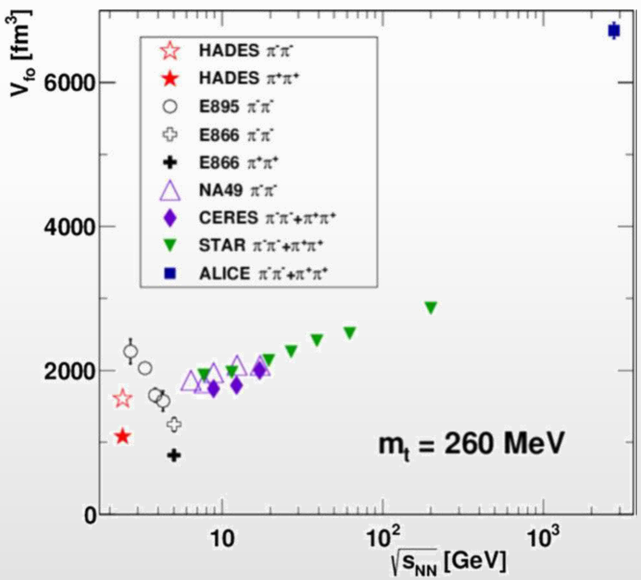

arXiv: 2209.01413 [nucl-th]

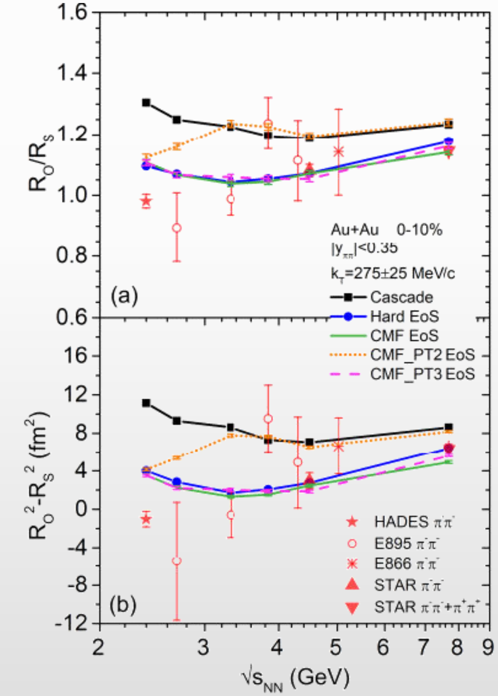

- Pion source radii are sensitive to the nature of the phase transition

Other observables …

- HBT measurements for identical particles
- Yield and flow of e+e- pairs:
  - ✓ probe deconfinement and chiral symmetry restoration
  - ✓ effective temperature

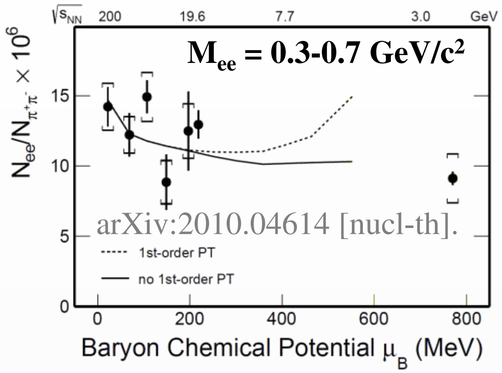

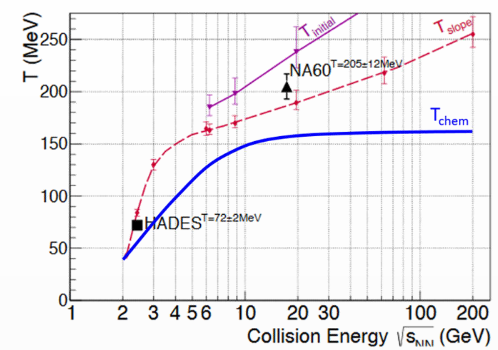

T. Galatyuk et al., Eur. Phys. J. A 52 (2016) 131; R. Rapp and H. v. Hess, PLB 753 (2016) 586
J.Cleymans et al. 2006 Phys. Rev. C73, 034905
NA60: H. Specht, AIP Conf. Proc. 1322 (2010) 160; HADES: Nature Physics 15 (2019) 1040

BiBi@9.2 GeV (UrQMD+PHSD), 10 M events→ full event/detector simulation and reconstruction

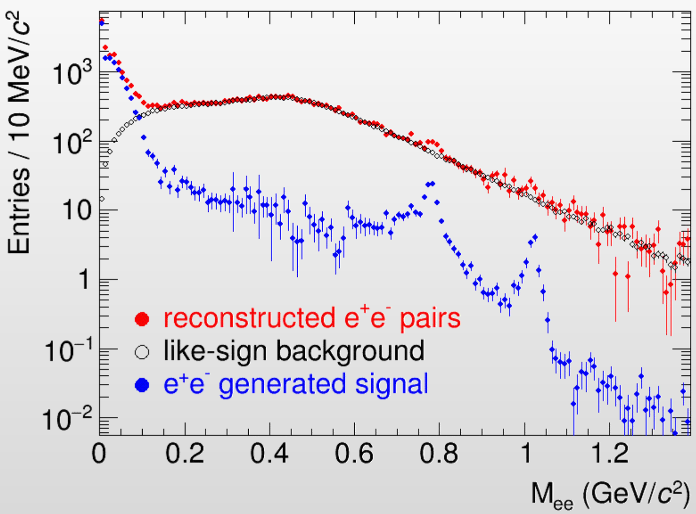

- S/B (integrated in 0.2-1.5 GeV/c2) ~ 5-10%
- Methods to improve S/B ratio with a minimal penalty for pair reconstruction are being developed
- Meaningful measurements for e^+e^- continuum and LVMs would require ~ 10^8 events, first observations will be possible with ~50 M events

Other observables …

- HBT measurements for identical particles
- Yield and flow of e+e- pairs
- Yields and flow of direct photons:
  - ✓ penetrating probe → direct (blue-shift-free) measure of the medium temperature over different evolution phases
  - ✓ scarce measurements at SPS, none at lower energies

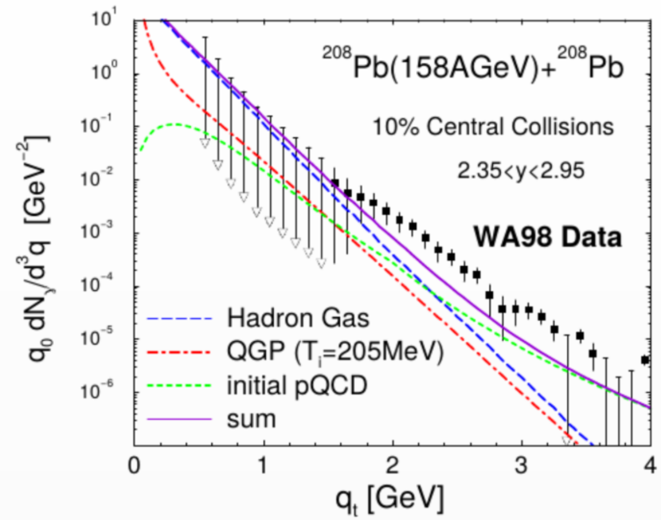

AuAu@11 (UrQMD), weak, but yet measurable signals are predicted for NICA energies

Physics of Particles and Nuclei, 2021, Vol. 52, No. 4, pp. 681–685

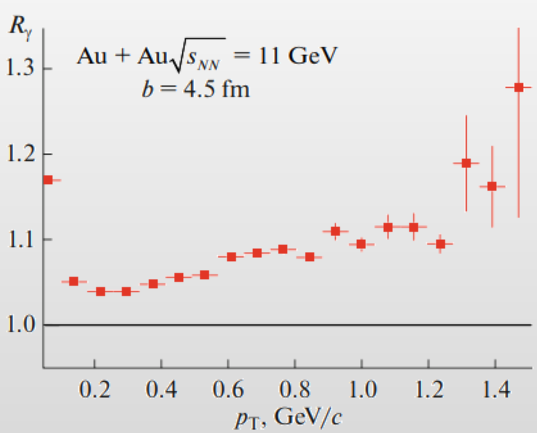

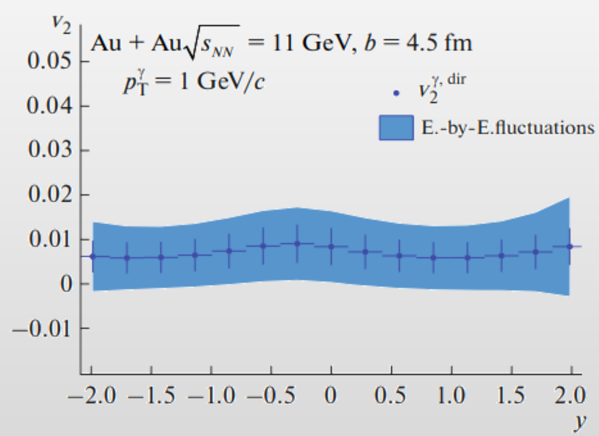

- ✓ ECAL and PCM for photon reconstruction and measurement of neutral mesons (background)
- ✓ Development of reconstruction techniques and estimation of needed statistics are in progress

Other observables …

- HBT measurements for identical particles
- Yield and flow of e+e- pairs vs. mass and momentum
- Yields and flow of direct photons
- Heavy-flavor production, search for exotic hadrons made of tetra- and penta-quark configurations:
  - ✓ statistics hungry analyses
  - ✓ some measurements require precise vertexing with internal silicon tracker foreseen for the MPD upgrade

Summary

- ❖ Preparation of the MPD detector and experimental program is ongoing, all activities are continued
- ❖ All components of the MPD 1-st stage detector are in advanced state of production
- ❖ Commissioning of the MPD Stage-I detector is expected in 2023
- ❖ Start of data taking with BiBi@9.2 in 2024
- ❖ Further program will be driven by the physics demands and NICA capabilities

BACKUP

Multi-Purpose Detector

Stage- I

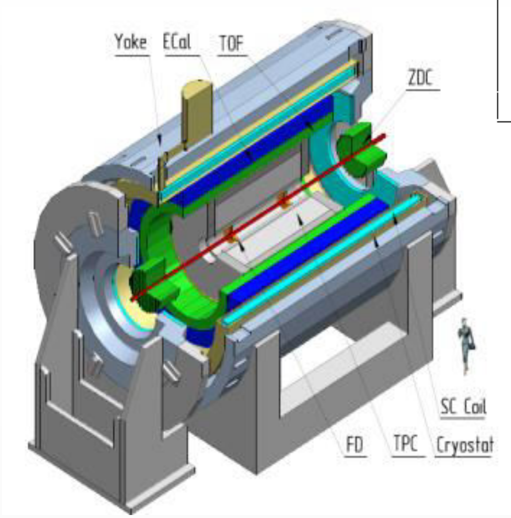

Length	340 cm
Vessel outer radius	140 cm
Vessel inner radius	27 cm
Default magnetic field	0.5 T
Drift gas mixture	90% Ar+10% CH_4
Maximum event rate	7 kHz ($L = 10^{27}$ cm^{-2}s^{-1})

upgrade

Stage- II

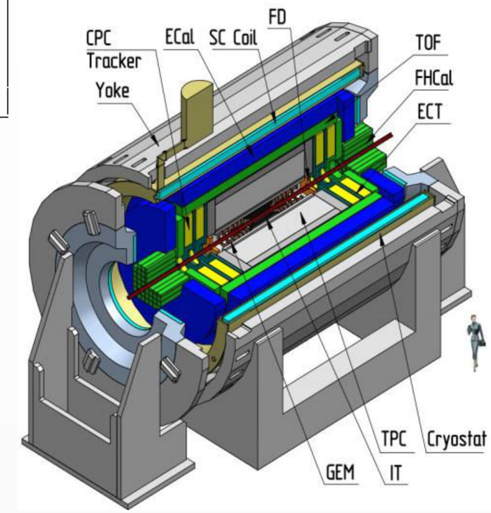

TPC: $|\Delta\varphi| < 2\pi$, $|\eta| \leq 1.6$
TOF, EMC: $|\Delta\varphi| < 2\pi$, $|\eta| \leq 1.4$
FFD: $|\Delta\varphi| < 2\pi$, $2.9 < |\eta| < 3.3$
FHCAL: $|\Delta\varphi| < 2\pi$, $2 < |\eta| < 5$

+ ITS (heavy-flavor measurements)
+ forward spectrometers

Au+Au @ 11 GeV (UrQMD + full chain reconstruction)

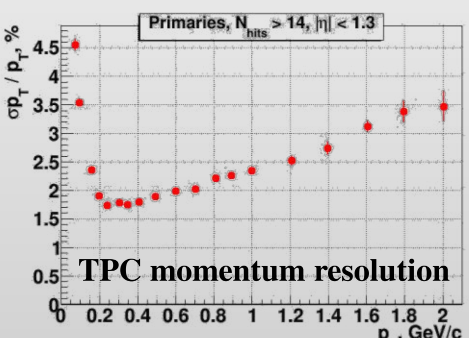

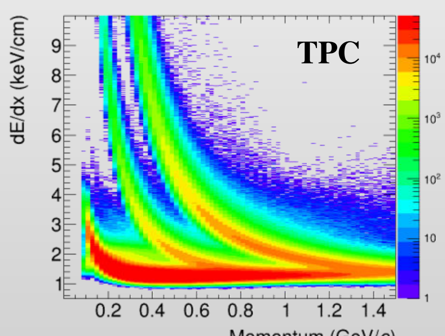

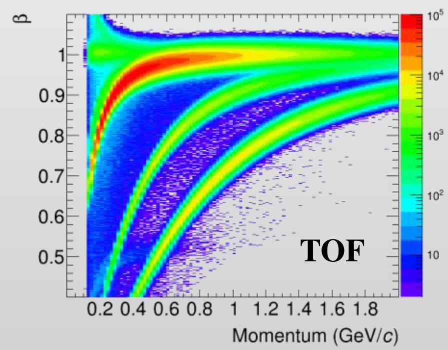

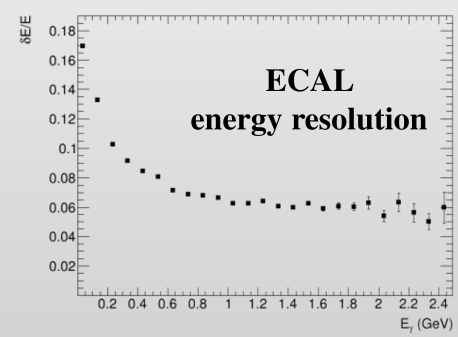

Support Frame for detectors inside of the Solenoid

The structure of Support Frame is made of carbon fiber which allows for deformation less than 3 mm under load with detectors (~80 T).
Producer - The Central Research Institute for Special Machinery, Khotkovo, Moscow region is a leading Russian enterprise in design and production of structures on the basis of advanced polymer composite materials for rocket & space engineering, transport, power, petrochemical machinery and other industries.

- the Frame will be transported to Dubna in November 2021
- December 2021 (as soon as Magnetic field measurements is finished)
- Representatives of the Company will participate in the process of installation of Support Frame into MPD and its alignment

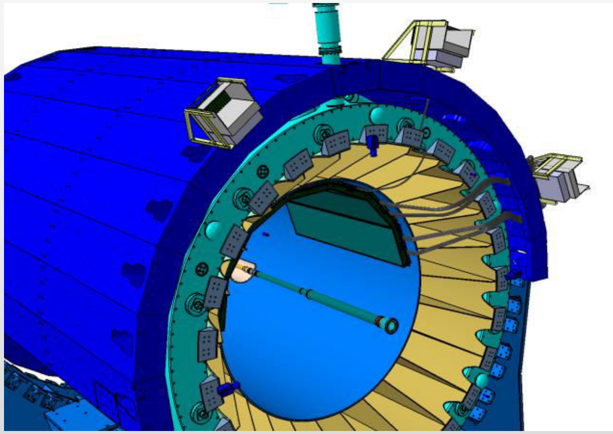

Time Projection Chamber (TPC): main tracker

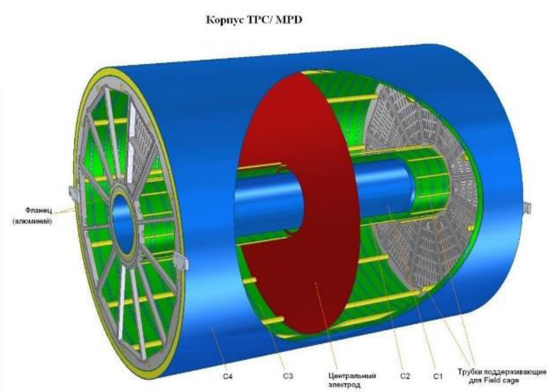

length	*340 см*
outer Radii	*140 см*
inner Radii	*27 см*
gas	*90%Ar+10%CH_4*
drift velocity	*5.45 см / μs;*
drift time	*< 30 μs;*
# R-O chamb.	*12 + 12*
# pads/ chan.	***95 232***
max rate	*< 7kGz (L= 10^{27})*

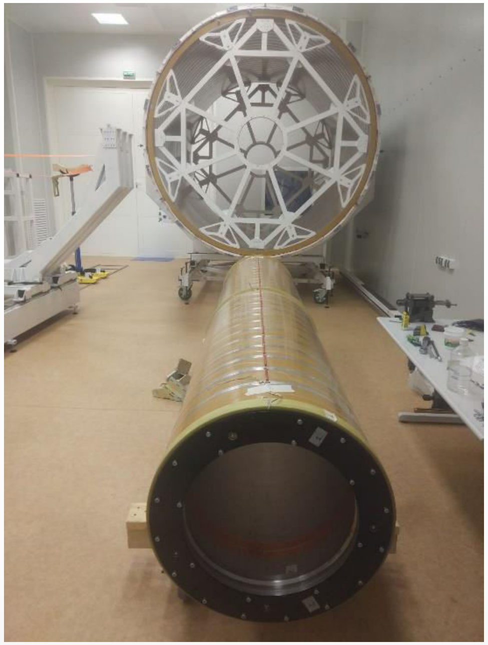

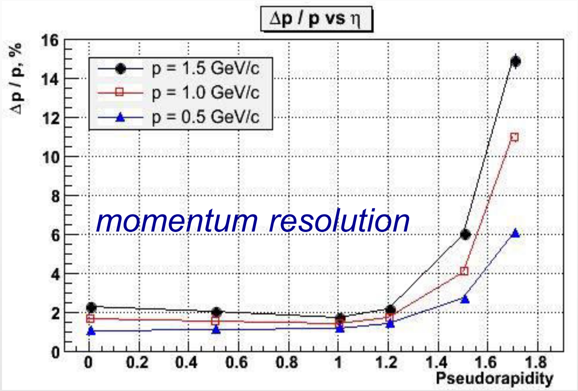

TPC/MPD Front-end card

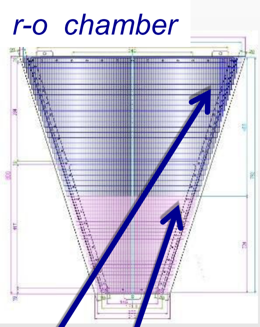

FE electronics: **FEC64SAM** –
*dual **SAMPA** card (**ALICE** technology)*

pad structure:
- *rows – 53*
- *large pads 5 × 18 mm^2*
-

Read-Out Chambers (ROCs) are ready and tested (production at JINR)
113 Electronics sets (8%) produced
Two sites (Moscow, Minsk) tested for electronics production
C1-C2 and C3-C4 cylinders assembled
TPC flange under finalization

MPD Time-of-Flight

Mass production staff: 4 physicists, 4 technicians, 2 electronics engineers
Productivity: ~ 1 detector per day (1 module/2 weeks)

Glass cleaning with ultrasonic wave & deionized water

Automatic painting of the conductive layer on the glass

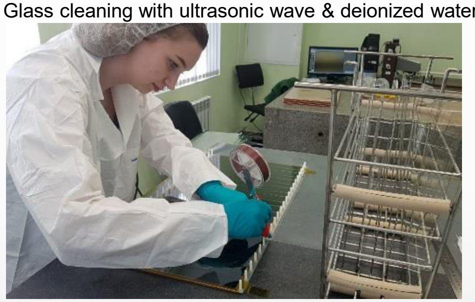

MRPC assembling

Soldering HV connector and readout pins

All procedure of detector assembling and optical control is performed in a clean rooms ISO class 6-7.

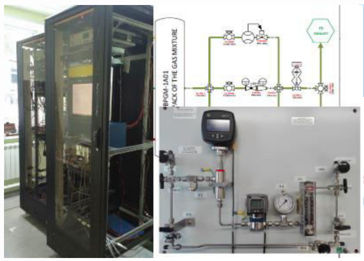

TOF gas system: Responsibility of the Polish group (WUT)

Dimensions of sensitive area 600 x300 mm^2

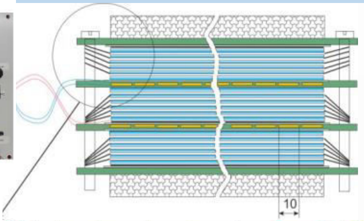

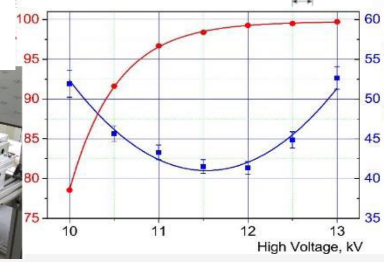

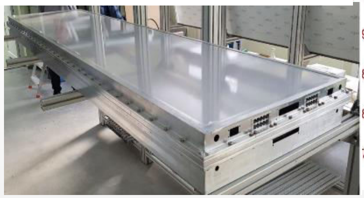

Single detector time resolution: 50ps

	Number of detectors	Number of readout strips	Sensitive area, m^2	Number of FEE cards	Number of FEE channels
MRPC	1	24	0.192	2	48
Module	10	240	1.848	20	480
Barrel	280	6720	51.8	560	**13440** (1680 chips)

Purchasing of all detector materials completed
So far 40% of all MRPCs are assembled
Assembled half sectors of TOF are under Cosmics tests
Investigation of solutions for detector integration and technical installations

Electromagnetic Calorimeter (ECAL)

- *Pb+Sc "Shashlyk"* *read-out: WLS fibers + MAPD* *L ~35 cm (~ 14 X_0)*
- *Segmentation (4x4 cm^2)* *σ(E) better than 5% @ 1 GeV* *time resolution ~500 ps*

Barrel ECAL = <u>38400</u> ECAL towers (2x25 half-sectors x 6x8 modules/half-sector x 16 towers/module)

So far ~300 modules (16 towers each) = 3 sectors are produced
Another 3 sectors are planned to be completed by May 2021
Chinese collaborators will produce 8 sectors by the end of 2021
25% of all modules are produced by JINR (production area in Protvino) 75% produced in China, currently funding is secured for approx. 25%

Projective geometry

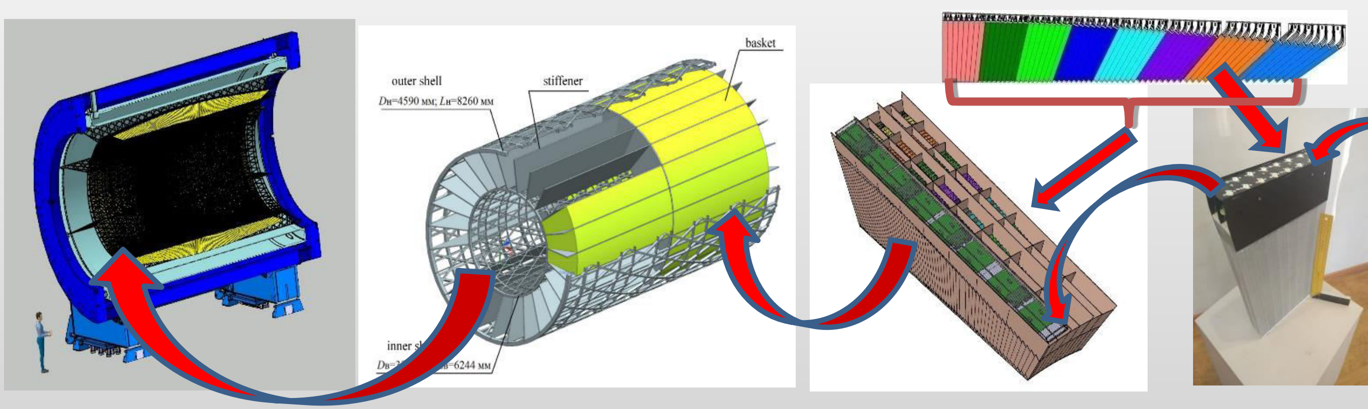

Sectors in dedicated Containers

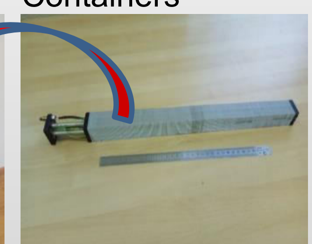

Photo of one tower

Forward Hadron Calorimeter (FHCal)

- All (90+spare) FHCal modules are assembled and are used for the tests.
- 100 Front-End-Electronics (FEE) boards are produced and tested.

The activities with modules:

- Tests with cosmic muons;
- Tests of Front-End-Electronics (FEE);
- Study of FEE electronic noises;
- Development of FHCal trigger;
- Development of Slow Control.

FHCal Trigger efficiency

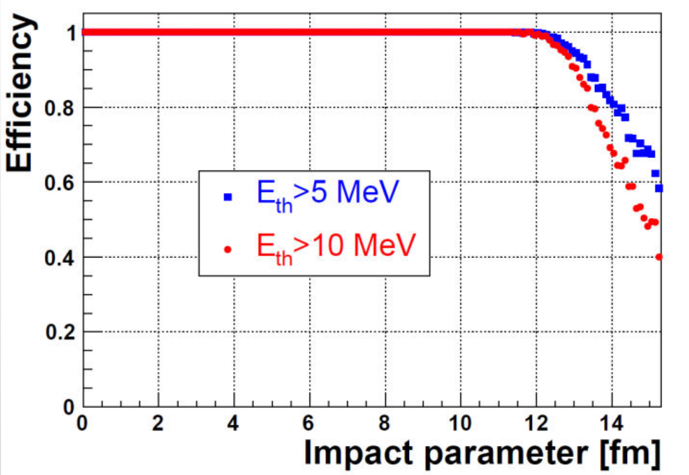

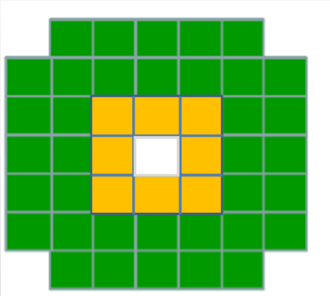

FHCal energy calibration with cosmic

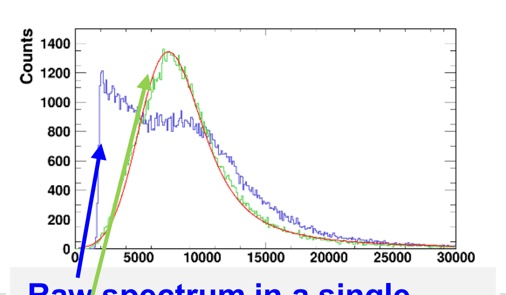

Raw spectrum in a single

Corrected to the pass length in scintillators

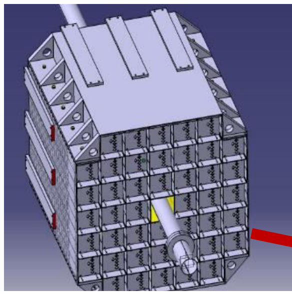

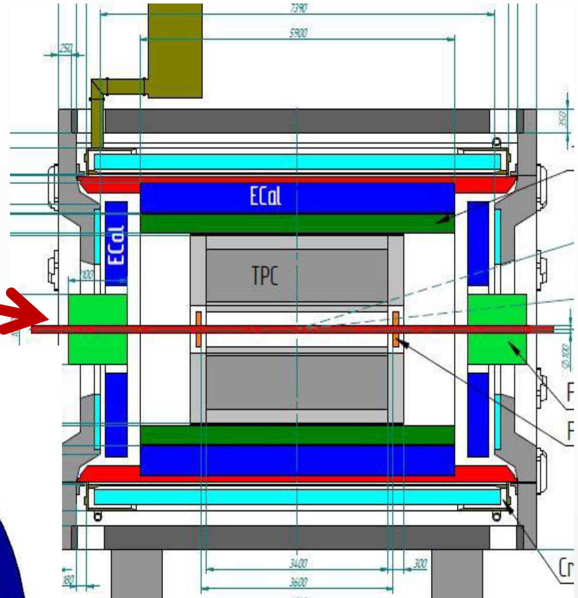

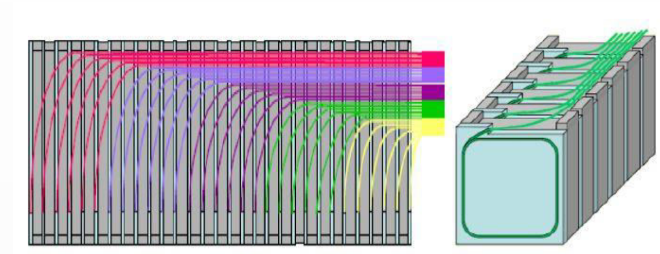

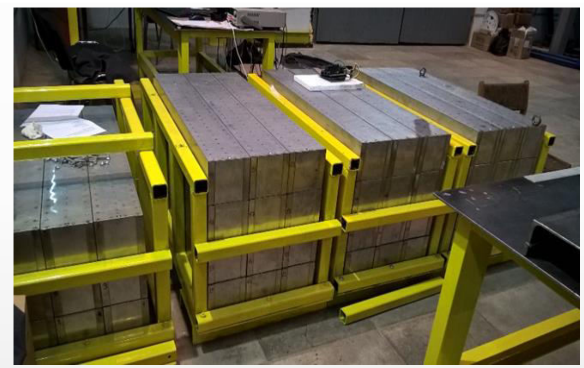

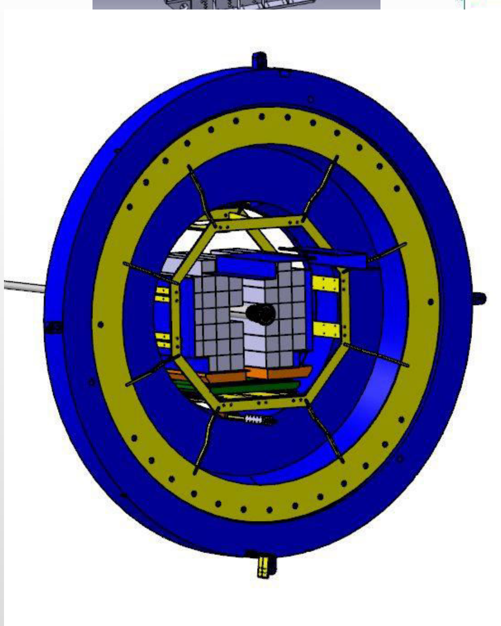

- **Two-arms at ~3.2 m from the interaction point.**
- **Each arm consists of 44 individual modules.**
- **Module size 150x150x1100cm^3 (42 layers)**
- **Pb(16mm)+Scint.(4mm) sandwich**
- **7 longitudinal sections**
- **6 WLS-fiber/MAPD per section**
- **7 MAPDs/module**

FFD - Fast Trigger L_0 for MPD

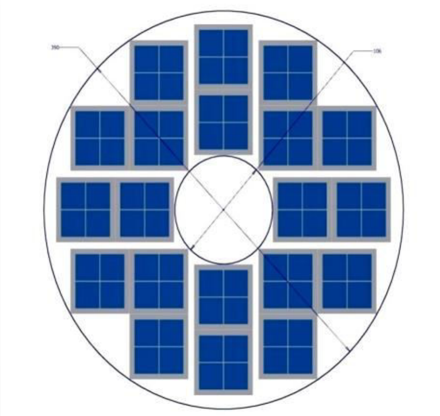

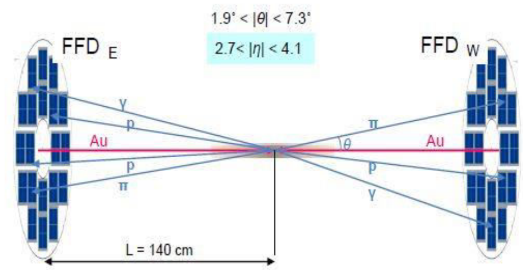

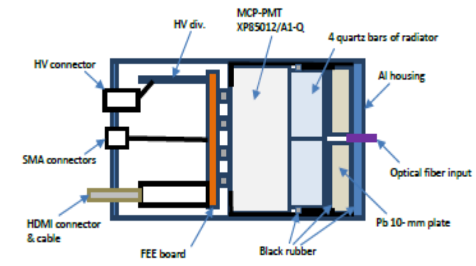

Fig. 4-1. A scheme of the FFD module.

FFD provides information on
- interaction rate (luminosity adjustment)
- bunch crossing region position

15 mm quartz radiator
10 mm Lead converter

The FFD sub-detector consists of
20 modules based on
Planacon multianode MCP-PMTs
80 independent channels

MPD trigger group is created on the basis of FFD team
Beside FFD we consider the signals from FHCal to be implemented into trigger L0
The FHCal team have produced trigger electronics.
Monte Carlo studies will be used to optimize the properties of the L0 trigger

Positioning of the NICA

- Data taking by STAR (PHENIX) at RHIC: $3 < \sqrt{s_{NN}} < 200$ GeV ($750 < \mu_B < 25$ MeV)

Au+Au Collisions at RHIC

Collider Runs						Fixed-Target Runs					
	$\sqrt{s_{NN}}$ (GeV)	#Events	μ_B	y_{beam}	run		$\sqrt{s_{NN}}$ (GeV)	#Events	μ_B	y_{beam}	run
1	200	380 M	25 MeV	5.3	Run-10, 19	1	13.7 (100)	50 M	280 MeV	-2.69	Run-21
2	62.4	46 M	75 MeV		Run-10	2	11.5 (70)	50 M	320 MeV	-2.51	Run-21
3	54.4	1200 M	85 MeV		Run-17	3	9.2 (44.5)	50 M	370 MeV	-2.28	Run-21
4	39	86 M	112 MeV		Run-10	4	7.7 (31.2)	260 M	420 MeV	-2.1	Run-18, 19, 20
5	27	585 M	156 MeV	3.36	Run-11, 18	5	7.2 (26.5)	470 M	440 MeV	-2.02	Run-18, 20
6	19.6	595 M	206 MeV	3.1	Run-11, 19	6	6.2 (19.5)	120 M	490 MeV	1.87	Run-20
7	17.3	256 M	230 MeV		Run-21	7	5.2 (13.5)	100 M	540 MeV	-1.68	Run-20
8	14.6	340 M	262 MeV		Run-14, 19	8	4.5 (9.8)	110 M	590 MeV	-1.52	Run-20
9	11.5	157 M	316 MeV		Run-10, 20	9	3.9 (7.3)	120 M	633 MeV	-1.37	Run-20
10	9.2	160 M	372 MeV		Run-10, 20	10	3.5 (5.75)	120 M	670 MeV	-1.2	Run-20
11	7.7	104 M	420 MeV		Run-21	11	3.2 (4.59)	200 M	699 MeV	-1.13	Run-19
						12	3.0 (3.85)	2000 M	750 MeV	-1.05	Run-18, 21

- MPD strategy – high-luminosity scans in **energy** and **system size**, looking for a wide variety of signals sensitive to the phase transition and presence of the critical point
- Scans to be carried out using the **same apparatus** with all the advantages of collider experiments

$dE_T/d\eta$ and $dN_{ch}/d\eta$

- Transverse energy and charged-particle multiplicity provide characterization of the nuclear geometry of the reaction, sensitive to dynamics of the colliding system (centrality, energy density, etc.)
- E_T/N_{ch} at NICA shows a quick increase of the average transverse mass of the produced particles

Phys.Rev.C 93 (2016) 2, 024901

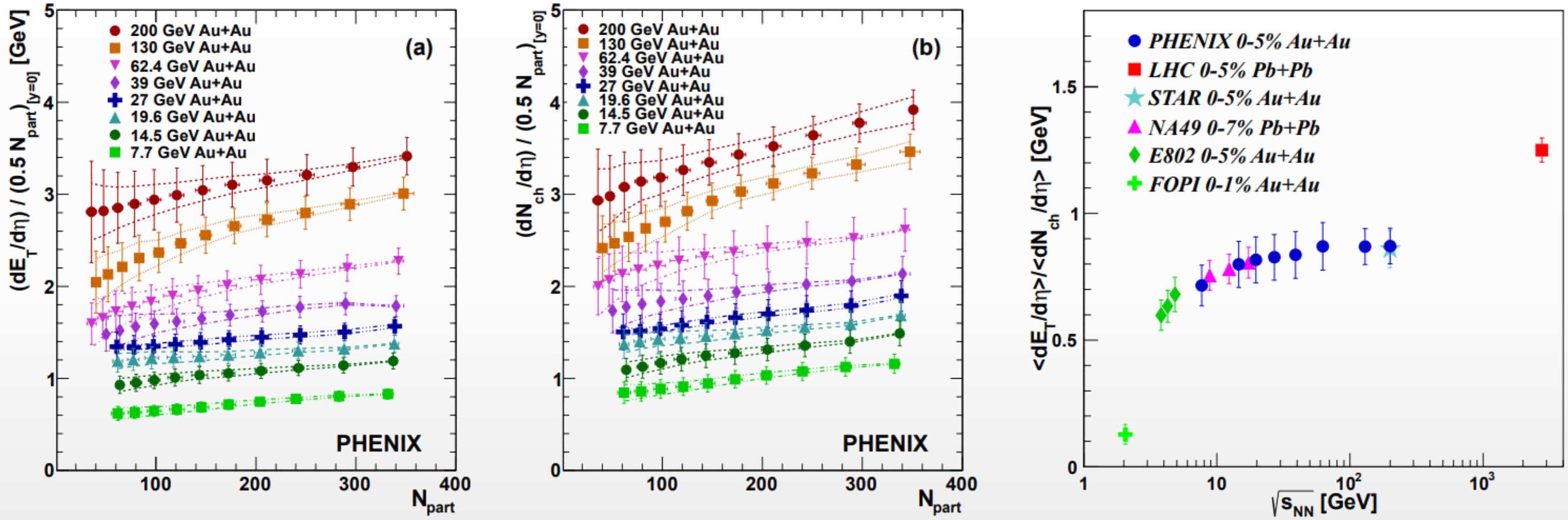

- Many references for cross-checks with other experiments
- The measurements will constitute the first physics results from the MPD

Why do we need new measurements at BM@N and MPD?

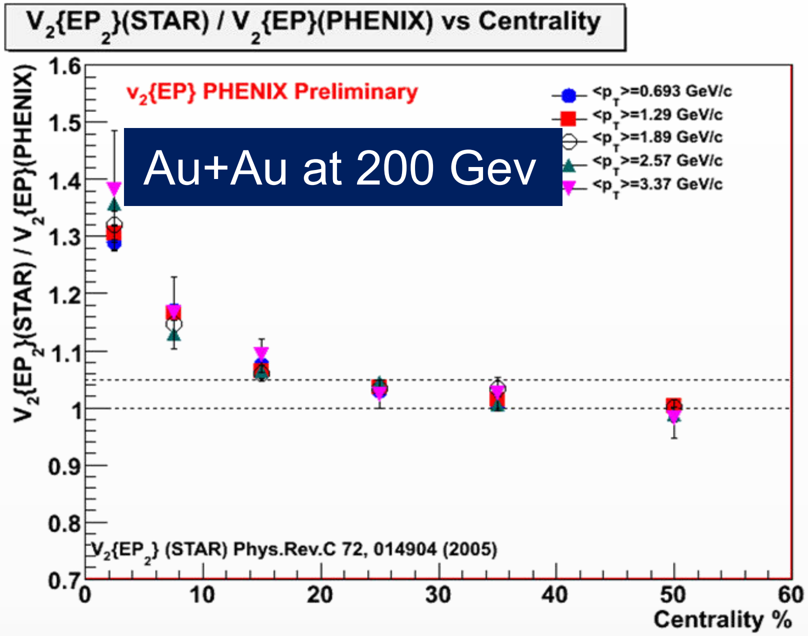

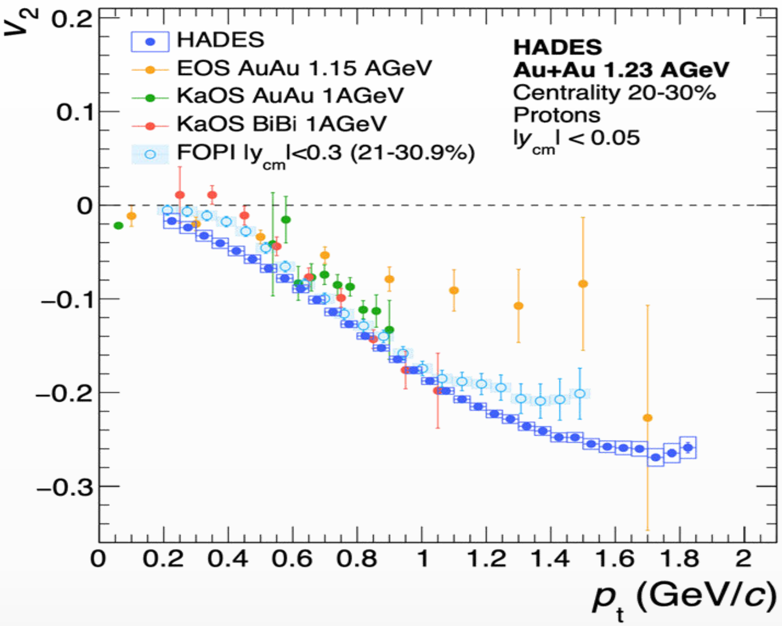

- ❖ The main source of existing systematic errors in v_n measurements is the difference between results from different experiments at the same collision energy
- ❖ A good measurement should be reproducible; in particular, it should be done in such a way that one can easily compare results from different experiments, using different detectors.

"Eliminating experimental bias in anisotropic-flow measurements of high-energy nuclear collisions", Matthew Luzum, Jean-Yves Ollitrault, Phys.Rev. C87 (2013) 4, 044907

GLOBAL BAYESIAN CONSTRAINTS ON QGP VISCOSITY

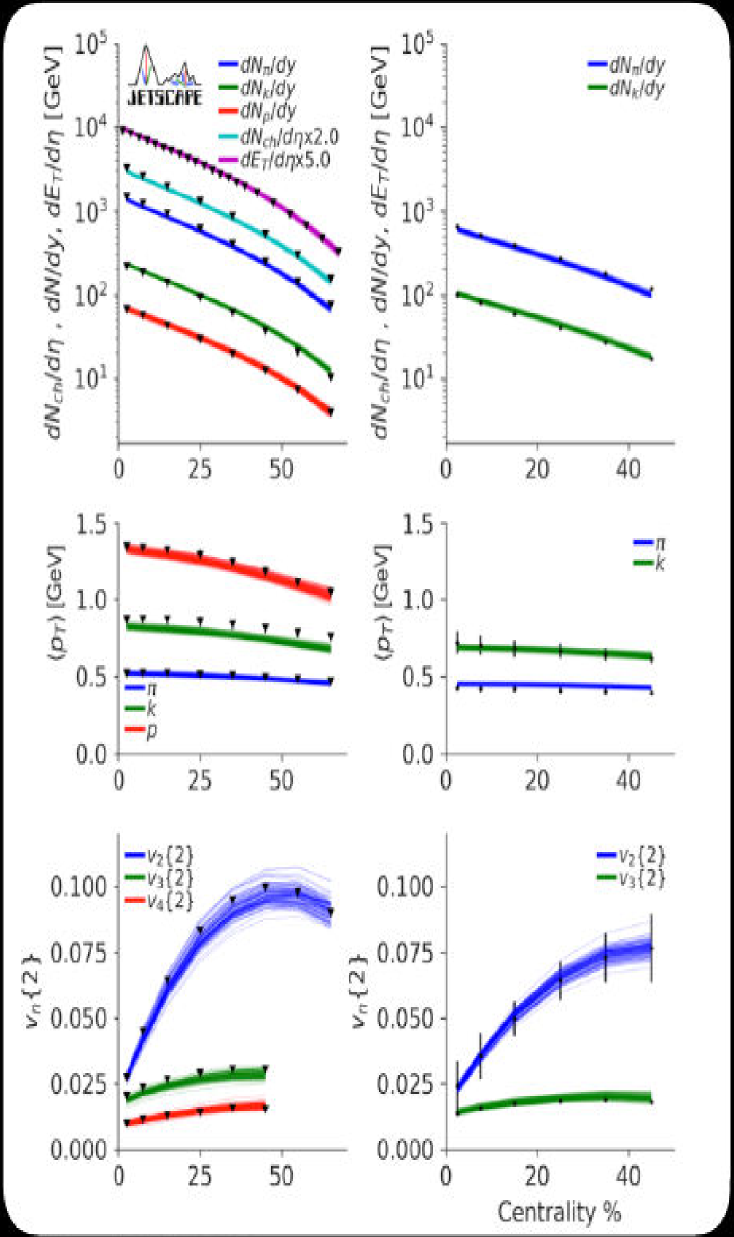

S. Pratt, E. Sangaline, P. Sorensen and H. Wang, Phys. Rev. Lett. 114, 202301 (2015)

J. E. Bernhard, J. S. Moreland, S. A. Bass, J. Liu and U. Heinz, Phys. Rev. C94, 024907 (2016)

J. E. Bernhard, J. S. Moreland and S. A. Bass, Nature Phys. 15, 1113-1117 (2019)

G. Nijs, W. Van Der Schee, U. Gursoy and R. Snellings,
Phys. Rev. Lett. 126, 202301 (2021) & Phys. Rev. C103, 054909 (2021)

D. Everett *et al.* [JETSCAPE], Phys. Rev. Lett. 126, 242301 & Phys. Rev. C103, 054904 (2021)

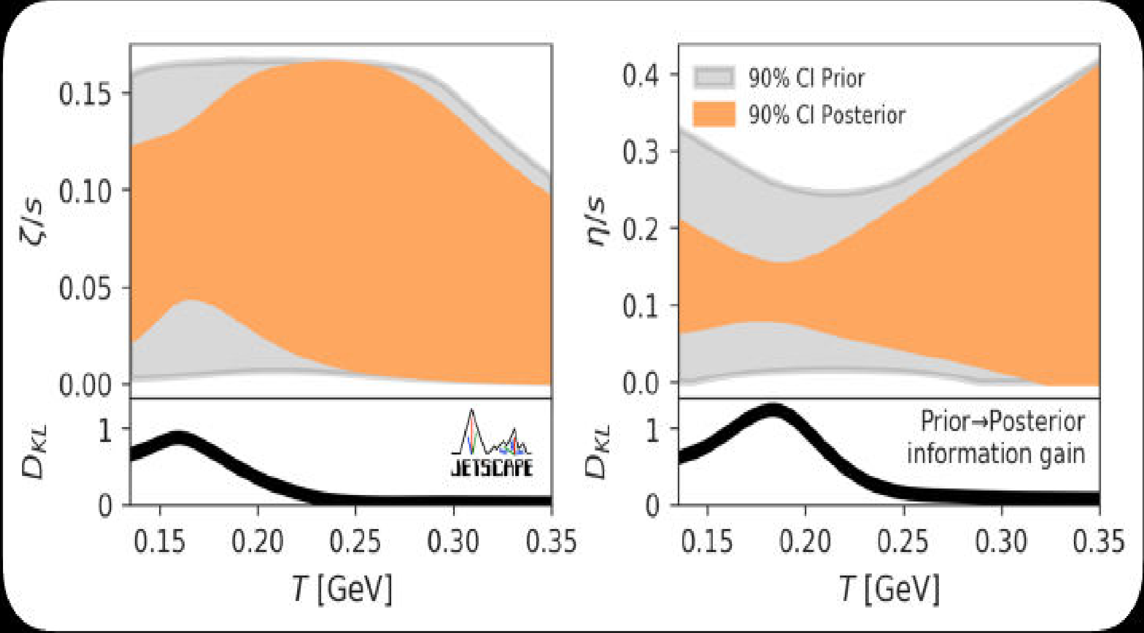

- Precision hadronic measurements can systematically constrain the QGP viscosity

Elliptic flow measurements using TPC: Scalar product, Event-plane

$$u_2 = \cos 2\phi + i \sin 2\phi = e^{2i\phi}$$

$$Q_2 = \sum_{j=1}^{M} \omega_j u_{2,j}, \ \Psi_{2,\mathrm{TPC}} = \frac{1}{2} \tan^{-1}\left(\frac{Q_{2,y}}{Q_{2,x}}\right)$$

- **Scalar product:** $v_2^{\mathrm{SP}}\{Q_{2,\mathrm{TPC}}\} = \dfrac{\langle u_{2,\eta\pm} Q^*_{2,\eta\mp}\rangle}{\sqrt{\langle Q_{2,\eta+} Q_{2,\eta-}\rangle}}$
- **TPC Event-plane:**

$$v_2^{\mathrm{EP}}\{\Psi_{2,\mathrm{TPC}}\} = \frac{\langle\cos\left[2(\phi_{\eta\pm} - \Psi_{2,\eta\mp})\right]\rangle}{\mathrm{R}_2^{\mathrm{EP}}\{\Psi_{2,\mathrm{TPC}}\}}$$

$$\mathrm{R}_2^{\mathrm{EP}}\{\Psi_{2,\mathrm{TPC}}\} = \sqrt{\langle\cos\left[2(\Psi_{2,\eta+} - \Psi_{2,\eta-})\right]\rangle}$$

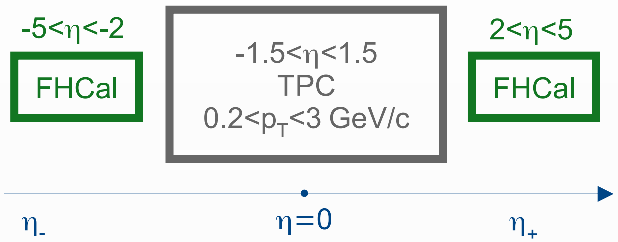

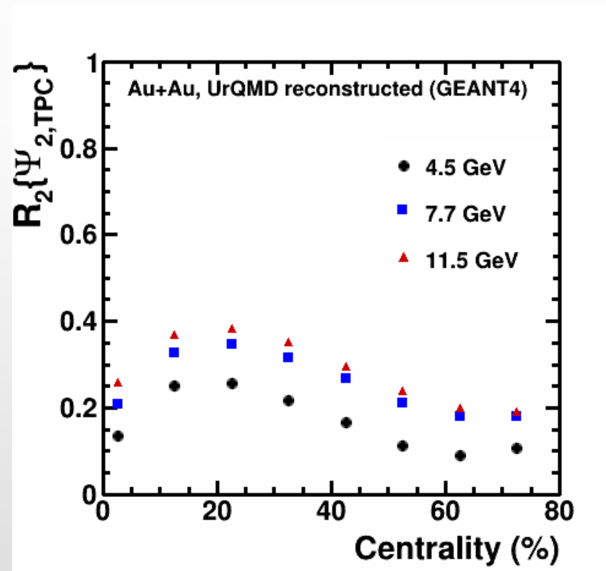

Elliptic flow measurements using TPC: Q-Cumulants

- **Standard Q-Cumulants:** (A. Bilandzic et al., Phys. Rev. C **83** (2011), 044913)

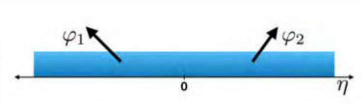

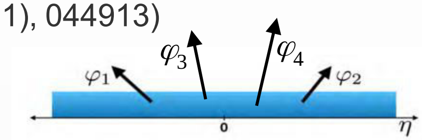

$$\langle 2\rangle_n = \frac{|Q_n|^2 - M}{M(M-1)} \approx v_2^2 + \delta \qquad \langle 4\rangle_n = \frac{[Q_n]^4 + [Q_{2n}]^2 - 2\Re[Q_{2n}Q_n^*Q_n^*] - 4(M-2)[Q_n]^2 - 2M(M-3)}{M(M-1)(M-2)(M-3)} \approx v_2^4 + 4v_2^2 + 2\delta^2$$

$$v_2\{4\} = \sqrt[4]{2\langle\langle 2\rangle\rangle^2 - \langle\langle 4\rangle\rangle}$$

δ – nonflow contribution

- resonance decay
- jets

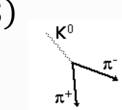

- **Subevent Q-Cumulants:** (J. Jia et al., Phys. Rev. C **96** (2017), no. 3, (

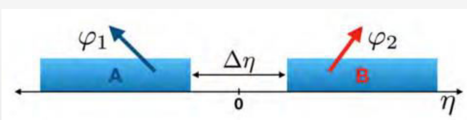

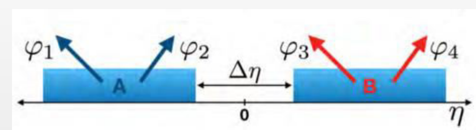

$$\langle 2\rangle_{a|b} = \frac{Q_{n,a}Q_{n,b}^*}{M_a M_b}, v_2\{2,2-\mathrm{sub}\} = \sqrt{\langle\langle 2\rangle\rangle_{a|b}} \qquad \langle 4\rangle_{a,a|b,b} = \frac{(Q_{n,a}^2 - Q_{2n,a})(Q_{n,b}^2 - Q_{2n,b})^*}{M_a(M_a-1)M_b(M_b-1)}, v_2\{4,2-\mathrm{sub}\} = \sqrt[4]{2\langle\langle 2\rangle\rangle_{a|b}^2 - \langle\langle 4\rangle\rangle_{a,a|b,b}}$$

Note: In this presentation, all of $v_2\{2\}$ result is obtained by subevent method to suppress non-flow contribution

Sensitivity of different methods to flow fluctuations

- Elliptic flow fluctuations: $\sigma_{v2}^2 = \langle v_2^2 \rangle - \langle v_2 \rangle^2$
- Assuming $\sigma_{v2} \ll \langle v_2 \rangle$ and a Gaussian form for flow fluctuations
- Fluctuations enhance $v_2\{2\}$ and suppress high-order **Q-Cumulants** compared to $\langle v_2 \rangle$:
- (S. A. Voloshin, A. M. Poskanzer, and R. Snellings, Landolt-Bornstein **23** (2010), 293)

$$v_2\{2\} \approx \langle v_2 \rangle + \frac{1}{2}\frac{\sigma_{v2}^2}{\langle v_2 \rangle} \qquad v_2\{4\} \approx v_2\{6\} \approx v_2\{8\} \approx v_2\{\mathrm{LYZ}\} \approx \langle v_2 \rangle - \frac{1}{2}\frac{\sigma_{v_2}^2}{\langle v_2 \rangle}$$

- **TPC EP method**: (M. Luzum et al., Phys. Rev. C **87** (2013) 4, 044907)

$$\langle v_2 \rangle \leq v_2^{\mathrm{EP}}\{\Psi_{2,\mathrm{TPC}}\} \leq \sqrt{\langle v_2^2 \rangle} \approx \langle v_2 \rangle + \frac{1}{2}\frac{\sigma_{v2}^2}{\langle v_2 \rangle}$$

- **Scalar product**:

$$v_2^{SP}\{Q_{2,\mathrm{TPC}}\} \approx \langle v_2 \rangle + \frac{1}{2}\frac{\sigma_{v2}^2}{\langle v_2 \rangle}$$

Simulation setup

- ✓ UrQMD v3.4 with hybrid model (3+1d hydro, **bag model** EoS, hadronic rescattering and resonances within UrQMD)
- ✓ π^0 and decay photon spectrum are calculated **within the same simulation**
- ✓ impact parameter range $0<b<9$ fm
- ✓ In hydrodynamical evolution, for each volume we calculate thermal gamma yield based on T, energy density (e), QGP fraction, baryonic chemical potential. We integrate these yields over time (until freeze-out time) and space.
- ✓ Two extreme cases: calculate thermal gamma emission from the volume above freeze-out criterion ($e > e_{freezeout}$), or calculate for all volumes. Reality somewhere in between (all volumes interact during hydro evolution). Comparing these options one can estimate theoretical uncertainties

$$\frac{d^3 N^{\gamma,therm}}{dy\, d^2 k_T} = \int_{\Omega} dV\, dt\, R_{\gamma}\left(k, T(x), \mu(x), u(x)\right)$$

Why simulations in PRC 93 054901 (2016) and PRC 81 044904 (2010) have almost the same yield despite ~5 times difference in energy (35 vs 158 AGeV)?

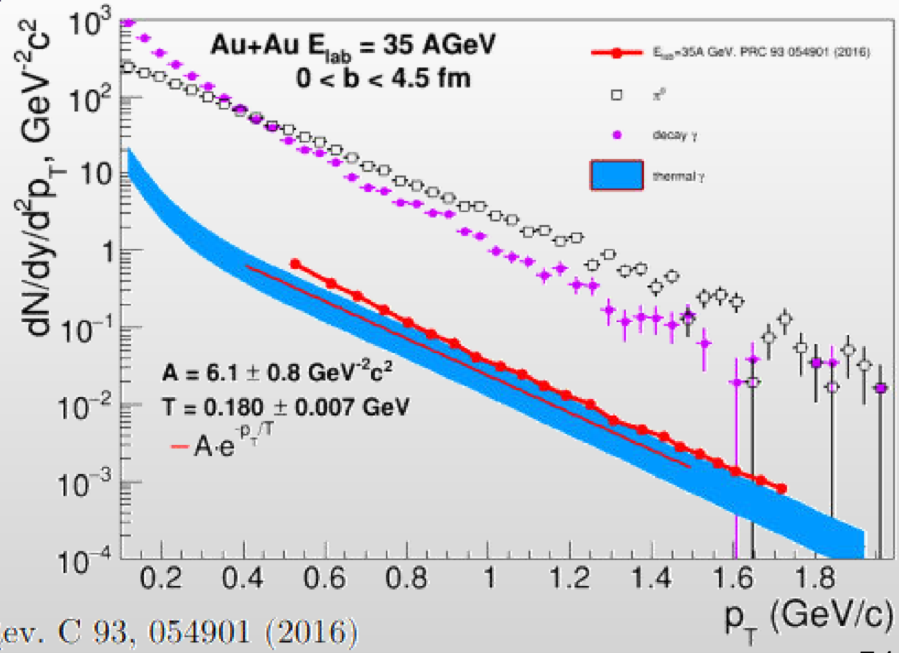

Comparison with S. Endres, H. van Hees, M. Bleicher, Phys. Rev. C 93, 054901 (2016)

Experimental challenges in fluctuations measurements

Event-by-event identification issues
- Cut based approach
- Identity method
- PSET identity method

Non-dynamical contributions
- E-by-e fluctuations of wounded nucleons
- Depends on centrality selection methods

Contributions from pileup events

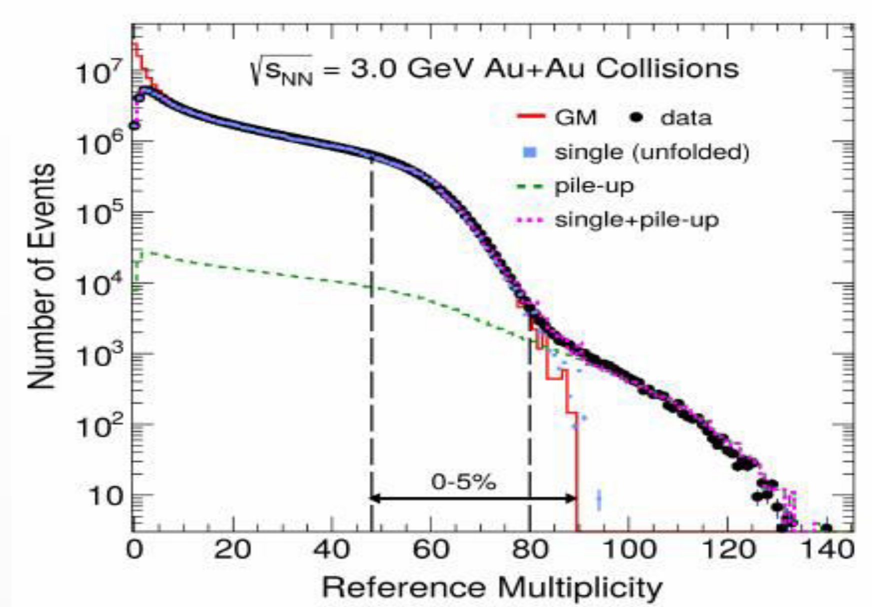

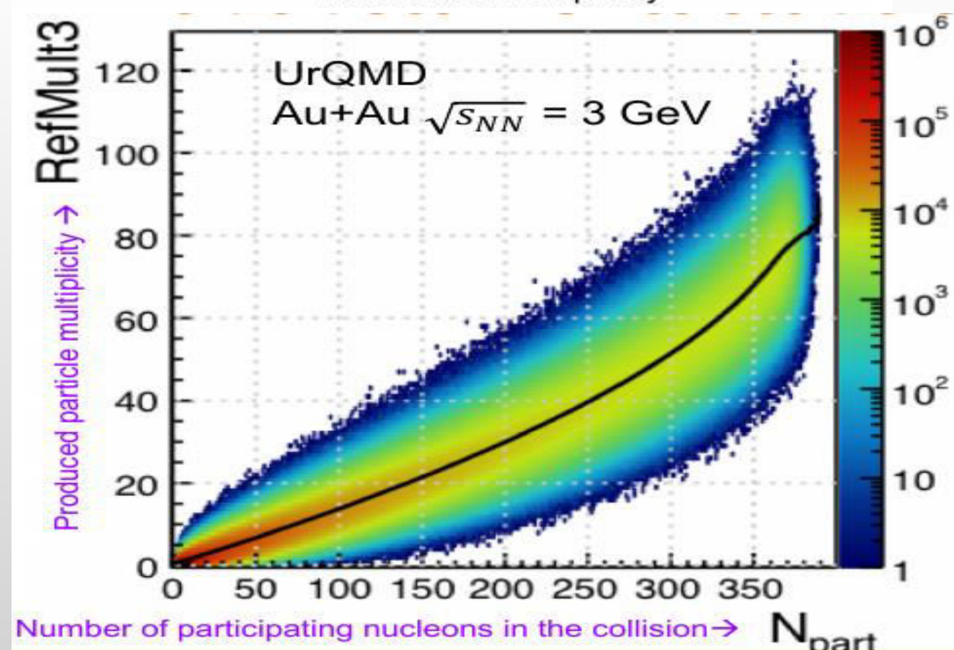

Finite-Size Effects and search for CEP

In HIC, both the size (**L**) and duration of formed system are finite.

Critical behavior changes with L

If the L is too small, the correlation length **ξ** can not be fully developed to cause a phase transition.

if the correlation length $\xi \sim |T - T_c|^{-\nu} \leq L$ the finite-size effect is not negligible and only a **pseudo-critical point, shifted from the genuine CEP, is observed.**

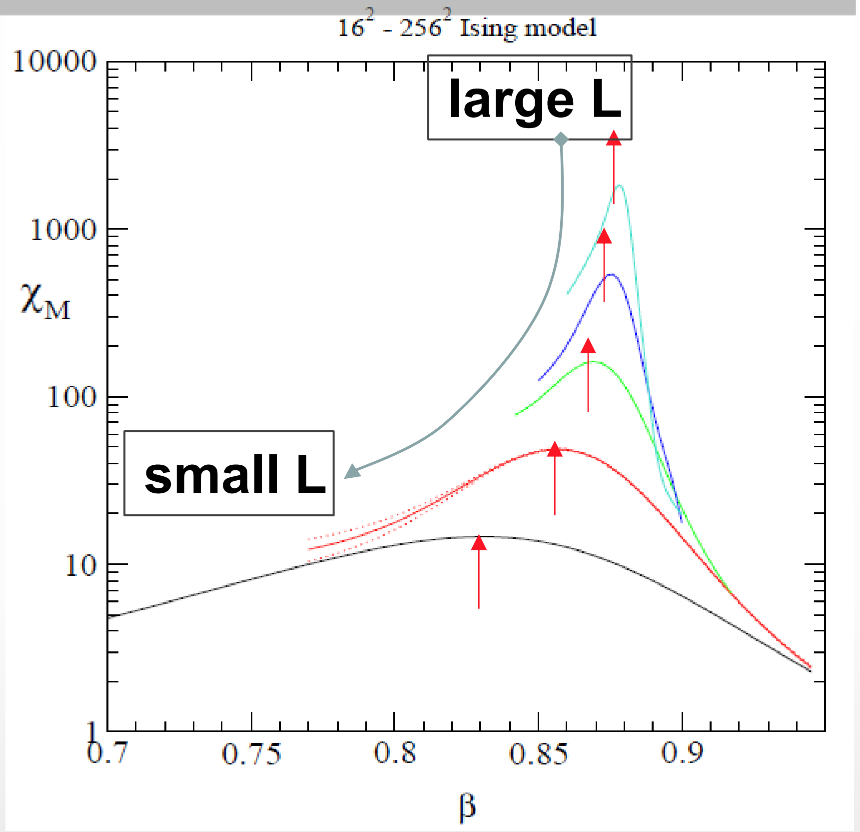

Note change in peak heights positions & widths with L

- ✓ **Finite-size effects have a specific dependencies on size (L)**
- ✓ **The scaling of these dependencies give access to the CEP's location, it's critical exponents and scaling function.**